
# Preliminary Studies with a Two-dimensional Model Using Transport Fields Derived from a GCM

I. G. Enting and J. V. Mansbridge

**DIVISION OF ATMOSPHERIC RESEARCH TECHNICAL PAPER No. 14**
COMMONWEALTH SCIENTIFIC AND INDUSTRIAL RESEARCH ORGANISATION, AUSTRALIA 1987

# Preliminary Studies with a Two-dimensional Model Using Transport Fields Derived from a GCM

By I. G. Enting and J. V. Mansbridge

Division of Atmospheric Research Technical Paper No. 14

Commonwealth Scientific and Industrial
Research Organisation, Australia
1987

*CSIRO Aust. Div. Atmos. Res. Tech. Pap.* No. 14, 1-47 (1987)

# PRELIMINARY STUDIES WITH A TWO-DIMENSIONAL MODEL USING TRANSPORT FIELDS DERIVED FROM A GCM.

By

I.G. Enting and J.V. Mansbridge

CSIRO, Division of Atmospheric Research
Private Bag 1 Mordialloc, Vic., 3195 Australia.

Presented at the CSIRO-ABM meeting on
'The Scientific Applications of Baseline Observations of Atmospheric Constituents'
Aspendale, November 7-9, 1984.

Abstract

This report describes some preliminary studies with a new two-dimensional atmospheric transport model. The transport fields were obtained from numerical experiments on a three-dimensional general circulation model and are not subjected to any tuning or calibration process.

The model is used to study the distribution of $CCl_3F$, $CO_2$ and $^{14}C$ in the atmosphere. It is found that the model's representation of the distribution of $CCl_3F$ in the troposphere is unsatisfactory. This is attributed to the excessively high tropical tropopause in the original GCM. The seasonal variation of $CO_2$ is modelled by using the surface concentrations to determine the surface sources and then using the model representation of the seasonal cycle at high altitudes as a test on the transport fields used in the model. The distribution of radionuclides from nuclear weapons testing is also modelled. These calculations compare reasonably well with observations except in the case of $^{14}C$ which has an anomalous seasonal behaviour.

## 1 Introduction

There have been a relatively large number of two-dimensional models developed for describing the distribution of minor constituents of the atmosphere. The distributions of such atmospheric tracers have been modelled in terms of atmospheric transports and sources and sinks for the various tracers. The transports are usually represented as due to a combination of zonal mean advection and a set of diffusion processes that purport to represent the effects of both transient eddies and standing eddies that can not be represented in a two-dimensional formulation. A major difficulty in setting up a two-dimensional model is the choice of appropriate values of these transport fields.

There are several ways in which transport fields can be obtained. The main possibilities are:

i Direct observations
ii Theoretical inferences from direct observations
iii Calibration of transport fields from observations of tracer distributions
iv Numerical determination of effective transport coefficients from calculations using general circulation models.

Each of these approaches suffers from severe limitations and in practice some combination is generally used. Direct observations are generally possible only for the advective transports and even in this case there are relatively few data for the southern hemisphere. More importantly, direct observations determine an Eulerian mean for the zonal mean transports. The use of Eulerian means is correct only if the diffusive transports are represented by diffusion tensors that are asymmetric, thus creating additional problems for other aspects of determining the transport fields.

The approach of using theoretical inferences to estimate transport coefficients has mainly been used in the determination of diffusive transports by assuming some fixed relation between the effective diffusion and certain statistical properties of the variability of the wind fields. This approach is of doubtful theoretical validity and has not been subjected to any validation studies on a global scale.

The use of tracer distributions to determine the transport coefficients (or to tune a set of initial estimates) suffers from the limitation that this calibration problem is severely underdetermined. In particular, there are very few atmospheric constituents for which the sources and sinks are known sufficiently well to form the basis for this sort of calibration. There is a real danger of developing circular arguments when it becomes necessary to use observations of a single tracer to deduce both the transport coefficients and the sink strengths.

The use of transport coefficients derived from a general circulation model provides a possible way of escaping from these limitations and it is this approach that is investigated in this report. The transport coefficients were derived by Plumb and Mahlman (1987) from the GFDL (Princeton) GCM/tracer model (Mahlman and Moxim, 1978). Plumb (1985) described a number of studies that test how well a two-dimensional representation can reproduce the results of experiments performed using the original GCM. The present report describes studies that must be regarded as merely preliminary for several reasons. Firstly, the transport fields that were used in this study were only preliminary values (Plumb, personal communication). In particular, the effects of small-scale vertical diffusion processes in the original GCM were not included. Secondly, our representation of these transport fields is only preliminary. Subsequent

studies, to be reported elsewhere, have indicated that alternative representations of the stream functions are preferable to those used here.

Section 2 of the present report reviews two-dimensional modelling in terms of the development of improved representations of the transports. The rest of the report investigates the question of how well the two-dimensional transport fields from the GCM/tracer model can reproduce observed distributions of minor atmospheric constituents. The use of a two-dimensional representation is not the only way of using GCM transport fields in the study of tracer distributions. The transport fields from GCMs have been used to study tracer distributions in three-dimensional models by Mahlman and Moxim,(1978), Levy et al. (1979), Fung et al. (1983) and Fung (1985) (see also Fung et al., 1985; Prinn and Golombek, 1985 and Prather, 1985).

The advantages of using two-dimensional models compared to three-dimensional models are that with a smaller model it becomes practical to perform a systematic investigation of a much larger range of mechanisms for the sources and sinks of particular tracers. In addition, should it become necessary to tune the model to allow for any limitations in the original GCM, this tuning process does not appear to be of unmanageable complexity, unlike the prospect of tuning the transport coefficients of a three-dimensional model. It should be possible to develop stable calibration techniques based on techniques of constrained inversion. The difference from case (iii) above is that the GCM-based transport field should provide a good initial guess that can be subjected to minor refinements as necessary; by constraining the refinements to be small a stable tuning scheme should be achievable.

As a basis for this type of study, the present paper describes a number of direct studies for particular tracers. The calculations were performed using a new two-dimensional transport model which is described briefly in Section 3. In Section 4, $CCl_3F$ is studied, primarily as a check on the amount of interhemispheric transport in the model.

The seasonal variation of carbon dioxide is studied in Section 5. This problem is more complicated because no attempt is made to model the surface sources and sinks. In the model, the surface concentrations are forced to follow the observed behaviour. The seasonal variations above the surface are used as a check on the validity of the transport formalism. In addition this calculation provides a way for estimates of surface source strengths as a function of latitude and time to be calculated directly (as opposed to the iterative procedures used by Pearman and Hyson, 1980). This treatment of the seasonal variation of $CO_2$ is justified on the basis of an argument based on Green's functions.

Finally, in Section 6, the model is used to investigate the transport of the products of nuclear testing from the stratosphere to the troposphere. While many of the radionuclide distributions can be represented adequately by the model, the seasonal variations of $^{14}C$ over the period 1962-1966 are anomalous. There have been a number of conflicting explanations of this seasonal behaviour by various workers of the last 20 years. While the present calculations can exclude some of these possibilities, it has not been possible to obtain a satisfactory model for the behaviour of $^{14}C$.

## 2 Transport Fields Used In Other Modelling Studies

This section briefly reviews the development of refinements to the way in which two-dimensional transport models of the atmosphere have been formulated. The main aspect of these developments concerns the role of the off-diagonal diffusion coefficients. This evolution has been reviewed by, for example, Matsuno (1980) and Brasseur and Solomon (1984). The aim of the present section is to show how this evolution in concepts has influenced modelling studies in CSIRO.

In order to describe the development it is useful to make a distinction between the formal mathematical description of the transports and the description that is actually used in computation. The general mathematical expression gives the transport as the sum of an Eulerian mean circulation and a general diffusive contribution involving 4 independent fields of transport coefficients. This type of expression is called 'K-theory' and arises from taking the lowest-order closure for describing the turbulent fluxes (see for example Peters and Carmichael, 1984). This general formalism is usually modified by using the fact that any anti-symmetric component of the diffusion tensor is mathematically equivalent to an additional advective flux. Thus most computational formulations use symmetric diffusion tensors and make the appropriate adjustment to the Eulerian mean advection.

There have been three main stages in the development of the application of 'K-theory' to atmospheric transport.

(i) Originally, Reed and German (1965) presented arguments that implicitly assumed that the antisymmetric contribution to the diffusion tensor should be small. This implies that there is no need to make significant changes to the Eulerian mean advection for computational purposes.

(ii) Later work by Matsuno (1980), Clark and Rogers (1978), Wallace (1978), Plumb (1979) and Pyle and Rogers (1980) suggested that in fact the diffusion tensor should be dominated by the antisymmetric part in many parts of the atmosphere.

(iii) More specifically it has been suggested (see especially Matsuno (1980) and Plumb (1979) ) that the effective advection arising from the antisymmetric diffusion should almost cancel the Eulerian mean advection, particularly in mid latitudes and the stratosphere. This means that the final transport will arise from the small terms resulting from the cancellation of the largest contributions. The symmetric terms in the diffusion tensor are small and the effective circulation is small. This effective circulation is the appropriate quantity to use in transport calculations (within the assumptions of K-theory) but it has no widely accepted convenient name. The effective circulation is related to the Lagrangian mean circulation and in special cases (if the diffusion is along the isentropes) it is equivalent to the residual circulation defined by Holton (1981). For further details see Plumb and Mahlman (1987).

As remarked in the introduction, transport fields can be obtained from observations, deductions from observations, using tracers to calibrate models or from dynamical calculations. It is mainly the wind fields that can be determined from observations. The main compilations of such data are Newell et al. (1972), Oort and Rasmusson (1971) and Oort (1983). Variances

of observed wind fields can be used to deduce estimates of diffusion coefficients according to mixing length theory. This has been done by Reed and German (1965) and Luther (1975). The most common way to determine transport fields is to model the distributions of appropriate quantities and then tune the transport fields until the model results agree with the observations. Table 1 lists a number of studies of this type. Many of the transport fields deduced in these studies have subsequently been used by other workers. It should be noted that most other modelling studies include some degree of tuning of the diffusion coefficients and for any particular model this tuning has evolved with the model. The following descriptions review the development of several models with particular emphasis on the way in which improvements in the descriptions of the transports have been incorporated.

Table 1 Source of transport fields and origins of transport fields used in some modelling studies.

| Reference | Distributions fitted | Fields derived or tuned | Fields taken from other sources |
|---|---|---|---|
| Murgatroyd and Singleton (1961) | temperature | $\psi$ | |
| Louis (1974,1975) | temperature | $\psi$ | tropospheric $\psi$ (Newell et al.1972) |
| Louis (1974,1975) | ozone | K's | $\psi$ as above |
| Hidalgo and Crutzen (1977) | ozone, water | K's | $\psi$ (Louis, 1974) |
| Whitten et al. (1977) | ozone | K's | $\psi$ (Oort and Rasmusson, 1971) |

The first model considered is that of Hidalgo and Crutzen (1977). This model used wind fields from Louis (1974) and tuned the diffusion coefficients to give reasonable distributions of ozone and water vapour. Later versions of the model (Gidel et al., 1983) obtained refined estimates of the diffusion coefficients using the same two tracers. It should be noted that the stream functions used in this model are approximately Eulerian means in the troposphere (being based on the work of Newell et al. 1972, as used by Louis, 1974) while they are closer to the effective transport circulation in the stratosphere because they are based on Louis' inversion of the heat distribution.

The original form of the model developed by Hyson et al. (1980) was based on the use of the original Reed and German argument and so it used Eulerian mean circulations (from Oort and Rasmusson, 1971) and a symmetric diffusion tensor. The various versions of this model, developed within the Division of Atmospheric Physics (CSIRO, Australia), are referred to below as the 'old' model. The diffusion coefficients were originally based on those of Hidalgo and Crutzen (1977), but Hyson et al. increased them in many regions in order to give agreement with $CCl_3F$ distributions. It is interesting to note that Hyson et al. had to increase the diffusion coefficients given by Hidalgo and Crutzen even though the Hyson et al. model already had built in a numerical diffusion contribution arising from the use of a first-order upwind

differencing treatment of the advection. In certain regions the numerical diffusion was of similar magnitude to the diffusion coefficients tabulated by Hyson et al. In later work (Pearman et al. 1983) with this model, some of the ideas from (iii) above were implemented by setting the advection to zero in the stratosphere (i.e. assuming complete cancellation) and using only the diagonal diffusion coefficients. The most recent work (Pearman and Hyson, 1986) has used the same approach in the stratosphere and has used the more recent Eulerian mean circulations from Oort (1983) for the tropospheric advection.

A similar approach was taken by Isaksen and Rodhe (1978) (see also Rodhe and Isaksen, 1980). They also used the diffusion coefficients calculated by Hidalgo and Crutzen (1977) but took the wind fields from Newell et al. (1972) and Louis (1974).

A recent modelling study by Miller et al. (1981) took a different approach. They used advective fields that were expected to directly represent the residual circulation. These fields had been calculated by Murgatroyd and Singleton (1961) directly from the temperature distribution in the stratosphere, assuming that any imbalance between source and sinks of heat was due solely to a purely advective transport of heat. Miller et al. applied a correction factor to these fields because more recent work had refined the atmospheric heating rates used by Murgatroyd and Singleton. Miller et al. also supplemented the advective transport by diffusion coefficients taken from Luther (1975) and Hunten (1975). In spite of the apparent inconsistency between the assumptions used in deriving the advection and the assumptions used in deriving the diffusion, the combined transport formulation appeared to give a good description of the distribution of various long-lived tracers in the stratosphere.

Other two-dimensional models have been described by Widhopf and Giatt(1980) and by Clough (1980) and Derwent and Curtis (1977) using combinations of stream functions from Louis (1974) and Newell et al. (1972) and diffusion coefficients from Louis (1974) or Luther (1975). All of the models mentioned above have been used in a variety of studies of different tracers - the details are beyond the scope of this section.

The main aim of the present paper is to validate the use of the GCM-based fields in transport modelling. In order to do this the results of the GCM-based calculations are compared to observations of the distributions of various tracers. In addition to these comparisons, a number of comparisons are made with the results of calculations using Eulerian mean circulations combined with symmetric diffusion tensors. Some of these calculations were performed using the older model described by Hyson et al. (1980). Other calculations were performed by using the new model described in Section 3 with the transport fields given by Hyson et al.. This type of comparison is limited because, as described in Section 3, the new model does not reproduce the numerical diffusion effects that occurred in the model of Hyson et al.. Some comparisons have been made by taking the same stream functions used by Hyson et al. and doubling the horizontal diffusion coefficients that they used as a first approximation to the actual behaviour of their model.

In order to indicate the differences in the formalisms, some of the fields used are plotted. Figure 1 shows a comparison of stream functions, comparing the GCM-based values for the effective circulation with the Eulerian mean circulation from Oort (1983) as used by Pearman and Hyson (1986). The differences between the Eulerian fields and the effective transport fields are quite pronounced. In particular the transport fields

have a single-cell circulation in each hemisphere unlike the Eulerian circulation which has two cells in each hemisphere.

Figure 2 shows a comparison of horizontal diffusion coefficients and Figure 3 shows a comparison of vertical diffusion coefficients. The GCM-based transport coefficients show a much larger vertical diffusion than was used in the 'old' two-dimensional model. The present studies indicate that the new $K_{pp}$ may be too large in that it gives too much transport between the stratosphere and the troposphere. In this regard, it has been noted (Plumb, personal communication) that the original GCM has its tropopause unrealistically high in the tropics. In each of the Figures 1 to 3 the plots are based on spectral expansions that are used by the new version of the model (see Section 3.2 below). In addition the various quantities have been converted into a common coordinate representation and common units. The stream functions shown in Figure 1 are mass-weighted stream functions in units of atmospheric masses per year. The horizontal diffusion coefficients in Figure 2 are in terms of y = sine(latitude) and are in units of earth radii squared per year. The vertical diffusion coefficients are in terms of height coordinates and are in units of scale heights squared per year.

The vertical diffusion coefficients represent the effects of eddy fluxes. The GCM also includes vertical fluxes due to small-scale diffusion and convection effects. These contributions were not available for the preliminary studies presented here. They are of most importance near the surface where the size of the eddies is restricted but are also significant in the mid troposphere in low to mid latitudes. In the calculations presented here these small scale effects were represented by setting a lower bound so that $K_{zz} \geq 5\ m^2\ s^{-1}$ (ie. $K_{pp} \geq 3.05p^2$ in dimensionless units) everywhere.

## 3 The Model

The numerical calculations presented in this paper were performed using a new two-dimensional transport model developed within the Division of Atmospheric Research (CSIRO, Australia). A brief description of some aspects of this model has been given by Enting (1984) and a more complete account is given by Enting and Mansbridge (1986). The present summary is divided into four parts: the numerical scheme used to represent the transport equation, the representation of the transport fields, the modes of operation of the model, and finally the relation between this model and the older two-dimensional model of Hyson et al. (1980).

### 3.1 Numerical Details

The transport is calculated using a finite-difference approximation to the two-dimensional advection-diffusion equation:

$$m \frac{\partial c}{\partial t} = \frac{\partial}{\partial x_1}\left[ m K_{11} \frac{\partial c}{\partial x_1} + (m K_{12} - \psi) \frac{\partial c}{\partial x_2} \right] + \frac{\partial}{\partial x_2}\left[ m K_{22} \frac{\partial c}{\partial x_2} + (m K_{21} + \psi) \frac{\partial c}{\partial x_1} \right] \qquad (3.1)$$

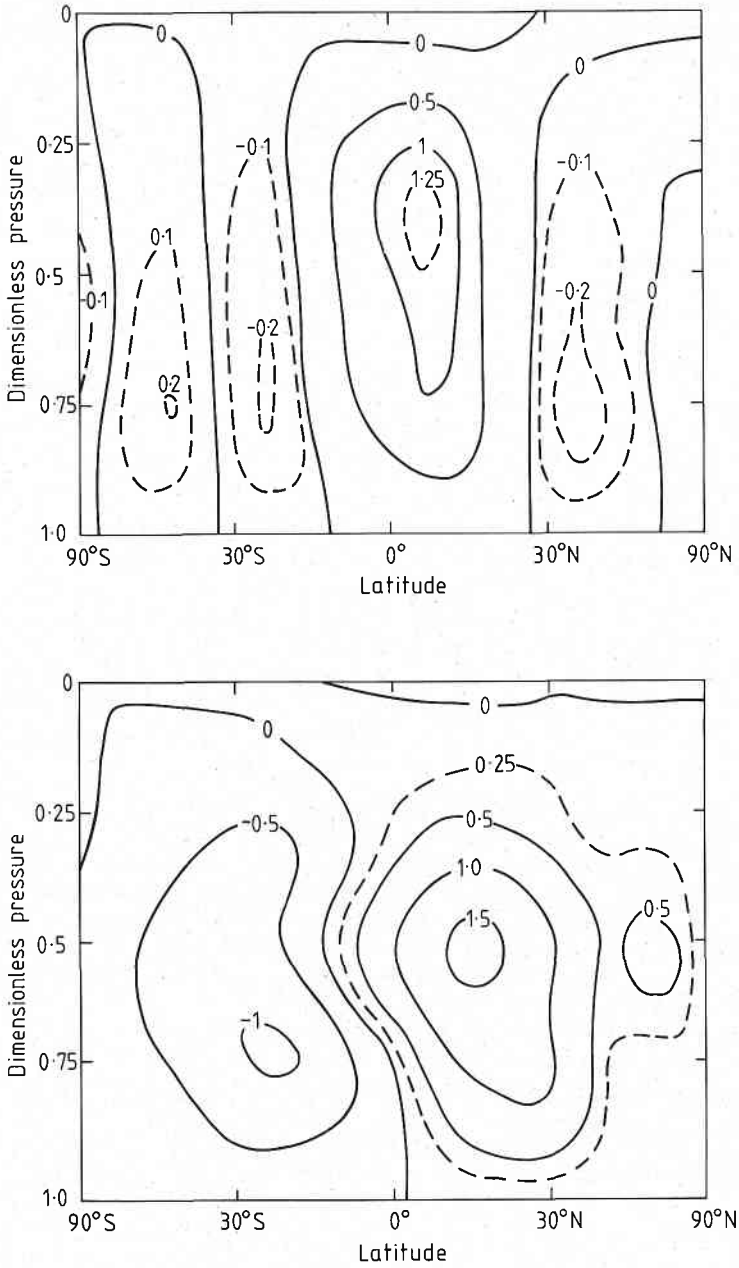


Fig 1: Comparison of stream functions used in the two-dimensional modelling. The Eulerian mean circulations are from Oort (1983) and are based on observations. The units are atmospheric masses per year. The effective transport circulations are from GCM calculations, (a) Eulerian mean, February. (b) effective transport circulation, February. (c) Eulerian mean, August. (d) effective transport circulation, August.

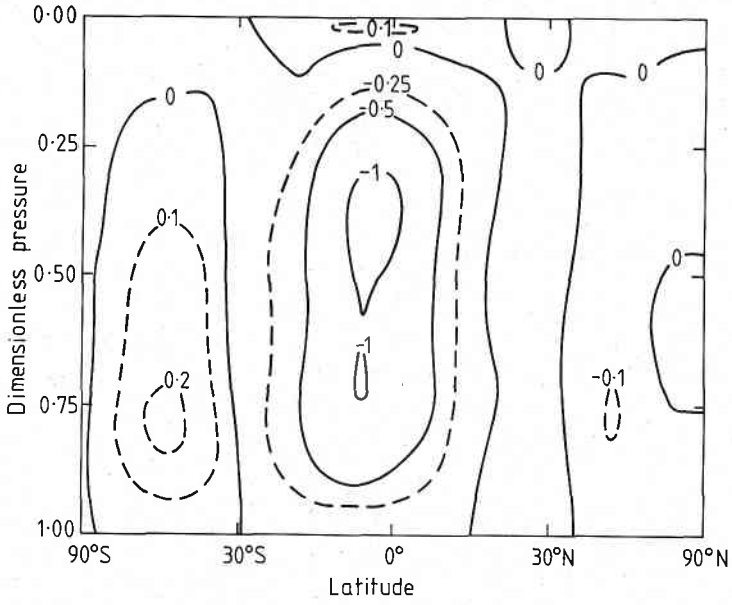
0·00
0·25
0·50
0·75
1·00
Dimensionless pressure
90°S
30°S
0°
30°N
90°N
Latitude
-0·1
0
-0·25
-0·5
-1
0·1
0·2
-0·1

(c)

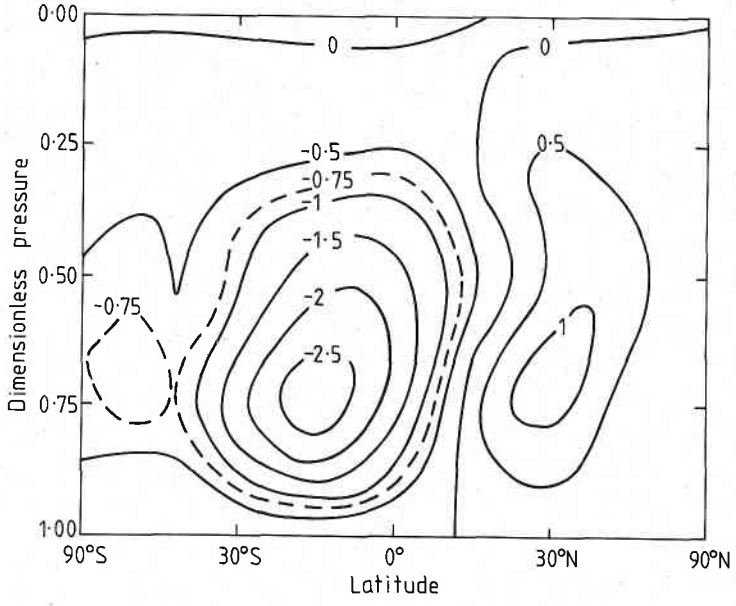
0·00
0·25
0·50
0·75
1·00
Dimensionless pressure
90°S
30°S
0°
30°N
90°N
Latitude
0
-0·5
-0·75
-1
-1·5
-2
-2·5
0·5
1

(d)

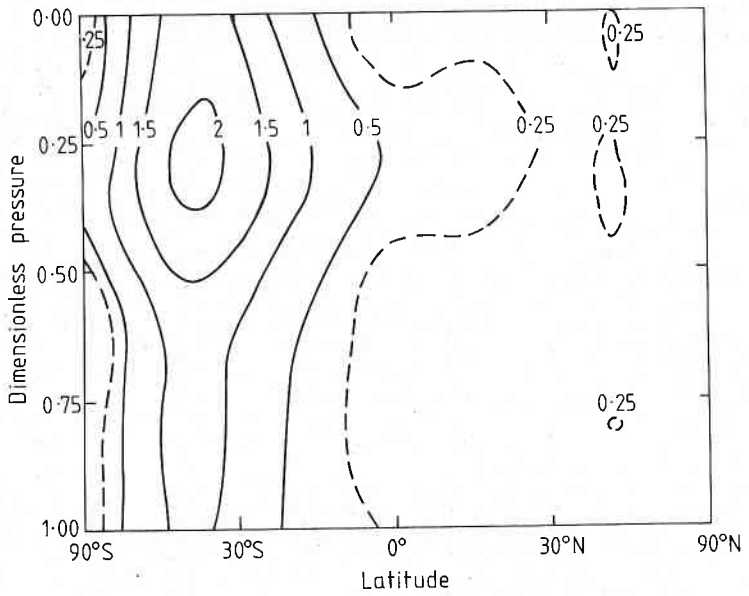


(a)

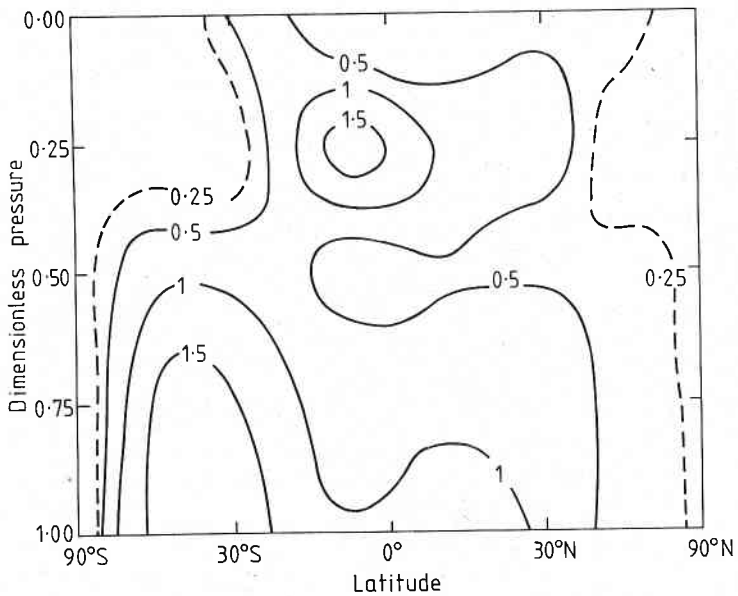


(b)

Fig 2: Comparison of horizontal diffusion coefficients, $K_{yy}$. The units are earth radii squared per year. The fields are shown for August when they have their maximum amplitudes. (a) Based on Hyson et al. (1980) (b) From GCM/tracer model.

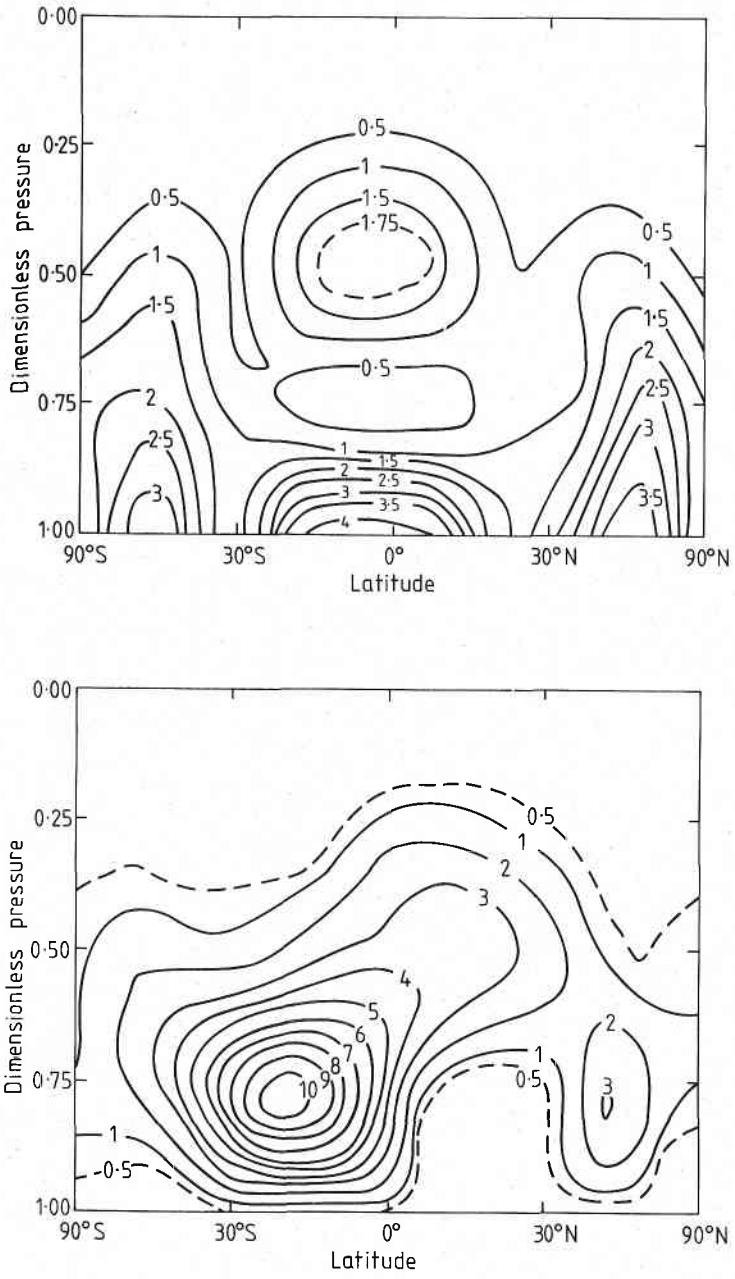


Fig 3: Comparison of vertical diffusion coefficients, $K_{pp}$. Units are scale height squared per year. The fields are shown for August when they have their maximum amplitudes. (a) Based on Hyson et al. (1980) (b) From GCM/tracer model.

where c is a tracer concentration,
$\psi$ is the mass-weighted stream function
m is the atmospheric density with respect to the x coordinates
and $[K_{ij}]$ is a diffusion tensor.

The diffusion tensor K is assumed to be symmetric. This is not actually a restriction because, as discussed in Section 2, it can be shown that any antisymmetric contribution to the diffusion can be treated as an additional contribution to the advective flow. The present model assumes that the transport fields have been transformed in this way before they are read into the model.

The program is set up so that the horizontal coordinate, $x_2$, can be $\phi$, the latitude, or $y=\sin\phi$. Similarly the vertical coordinate, $x_1$, can be either p, the (reduced) pressure or ln(p) representing a negative height. The model uses a grid that is equally spaced in terms of whichever coordinates are in use. The use of an equal pressure grid gives a good representation of the troposphere while the use of an equal height grid is better for resolving the stratosphere. The transport fields are transformed appropriately when they are read into the program. The number of grid points in each coordinate direction and the number of distinct tracers that are considered can be reset as desired, subject to the constraints of total available computer memory. All internal calculations are performed using the "dimensionless" units of years for time, earth radii for horizontal coordinates, scale heights for vertical distances and atmospheres for pressure. Tracer concentrations are represented in terms of mixing ratios (or multiples thereof) rather than densities. Masses of air are expressed in units of the total atmospheric mass. Conversions of vertical units between the p and ln(p) coordinates used in the model and actual heights or vertical distances are performed on the basis of an isothermal atmosphere with a scale height of 7.2km.

The spatial derivatives in Equation (3.1) are approximated by a centred differencing scheme which is essentially equivalent to that used by Miller et al. (1981). The time integration is performed using an Euler predictor-corrector method.

## 3.2 Details of the Transport Coefficients

The transport scheme requires four transport fields, $K_{11}$, $K_{12}=K_{21}$, $K_{22}$ and the stream function $\psi$. These fields are required to be specified as functions of time at the set of grid points that is appropriate for the particular choice of resolution and coordinates. (The coordinate values at which the transport fields are required are midway between the values at which the concentrations are specified in one or both directions.) The model meets these requirements by using transport fields that are specified in terms of a spectral expansion in both space and time. When the program is started the expansions are read and the spatial sums are evaluated at the necessary points. At each point this gives a Fourier series in time. This is summed at the midpoint of a selected interval (which can be as often as every time step) to give the coefficients that are actually used by the finite difference scheme.

The general representation of the transport fields is as a sum

$$f(p,x,t) = \sum_{k,m,n} g_k(p)\, g_m(x)\, g_n(2t) \qquad (3.2)$$

with
x = 0.5 (1 + sine(latitude))
p = pressure in atmospheres
t = time in years

and $g_k(z) = \cos(\pi kz) \quad k \geq 0$ (3.3a)

$= \sin(\pi kz) \quad k < 0$ . (3.3b)

The relevant range of each of the spatial coordinates is half of the period of the functions $g_k(z)$ that are used in the expansion. In order to specify a unique Fourier expansion it is necessary to define the behaviour of the functions f over the full period. This freedom is used to ensure that the derivatives of the functions are continuous to as high an order as possible; thus the most rapidly convergent series is obtained (Lanczos, 1966). For general fields, it is assumed that the function f is symmetric about each of its boundaries. This has two consequences: the function f will then be continuous at the boundaries and only non-negative indices for the spatial variation will be required. If the field goes to zero at the boundaries then the function f can be taken as being antisymmetric about each boundary. Then as well as the function being continuous at the boundaries its derivatives will also be continuous, and more rapid convergence of the series can be expected. For fields that go to zero on one pair of boundaries but not the other, the considerations above indicate that the appropriate expansion uses $k \geq 0$ for expansion of the spatial variability in one direction and $k < 0$ to expand the variability in the other direction.

The coefficients were determined by least squares fits to various sets of data defined on spatial grids. It was found necessary to exercise considerable care in choosing which functions to expand in order to obtain a reasonable representation throughout the atmosphere. Since least squares techniques minimise the sums of squares of absolute deviation rather than relative deviation, the representation can be relatively poor in regions where the transport fields are small. Since regions with small transport fields will correspond to 'bottlenecks' in the atmospheric mixing processes a failure to obtain a good representation of these regions can severely degrade the performance of the model. In order to minimise these problems the input fields that were taken as representing the transport fields from the GCM/tracer model were chosen as least squares fits of the form (3.2) to the following quantities:

i) $\psi/p$: (i.e. the velocity stream function). Taking least squares fits of $\psi$ was found to give a poor representation of stratospheric transports.

ii) $K_{zz}$: This field rather than $K_{pp}$, was chosen so as to give a good representation in the stratosphere.

iii) $K_{yy}$: The main regions in which this field is small are near the north and south boundaries at which it goes to zero. This behaviour can be ensured by using the sine expansion and so the least squares fitting procedure does not cause problems.

iv) $K_{yp}$: This field goes to zero on all boundaries, unlike the off-diagonal diffusion coefficients in other coordinate systems.

The model also has the facility to impose bounds on the coefficients to ensure that the diffusion does not become too small or even negative. This is achieved by specifying lower bounds for the diagonal components and upper bounds on the magnitudes of the off-diagonal components so that the diffusion tensor remains positive-definite. These bounds can be used to ensure

stability of the numerical scheme. In the present calculations the lower bound on $K_{zz}$ has been used to approximate the effects of the small scale diffusive and convective effects that were not included in the original fields obtained from the GCM/tracer model.

### 3.3 Modes of Operation

The transport scheme in the model can be regarded as evaluating the vector $\underline{Lc}$ where taking centred spatial differences has approximated Equation (3.1) by a model representation of the form:

$$\frac{\partial c_i}{\partial t} = \sum_j L_{ij} c_j + s_i \quad . \tag{3.4}$$

The normal way in which such a model is used is to take the transports specified by $\underline{Lc}$ and the sources specified by $s_i(t)$ and numerically integrate the set of Equations (3.4). An alternative use of the model occurs in the situation in which the concentrations are specified as (differentiable) functions of time. In this case it is possible to deduce the sources as functions of time by transforming (3.4) into

$$s_i = \frac{\partial c_i}{\partial t} - \sum_j L_{ij} c_j \quad . \tag{3.5}$$

While the case of knowing concentrations at all points is unlikely to occur with any real tracer, Enting (1984) has pointed out that it is possible to solve a mixed problem in which the grid points are divided into two classes. The first class is the set of grid points at which the sources are known and the concentrations are unknown. The second class is the set of grid points at which the concentrations are known and the sources are unknown. The concentrations at the first set of points are determined by numerically integrating (3.4). This integration will make use of the known concentrations from the second class. Once concentrations are determined at all points (either by numerical integration or because they were specified initially) Equation (3.5) can be used to determine the source strengths at the grid points in the second class. In Section 5 below this approach is used to determine the net surface sources of carbon dioxide given the variations of surface concentrations in space and time.

### 3.4 Relation to the Older Model

The main differences between the present model and the 'old' model described by Hyson et al. (1980) are

i) The new model gives a choice of coordinates and a choice of spatial resolution. Many of the calculations presented in subsequent sections use 8 layers and 10 zones.

ii) The new model uses diffusion coefficients that match the coordinate system that is in use, unlike the old model which uses $K_{zz}$ on what is predominantly an equal pressure grid and $K_{\phi\phi}$ on an equal y grid. The new model takes the spectral expansion defined on the p-y grid and evaluates the fields at equal intervals of p or z and y or $\phi$ as appropriate and then performs any necessary conversion of the diffusion coefficients.

iii) The new model uses mass stream functions rather than velocities to specify the advection. This reduces the storage requirements and automatically ensures the conservation of atmospheric mass.

iv) The new model uses a spatial differencing scheme that is correct to second order in the grid spacing. In contrast, the old model uses upwind differencing for the advective terms and is correct only to first order. The consequences of this are that the results of the old model depend more strongly on the resolution than would be the case with a higher order scheme. As part of this effect the upwind differencing scheme produces a 'numerical diffusion' (Noye, 1982) that is so large in certain critical regions that the effective diffusion coefficients may be more than 100% larger than the diffusion coefficients tabulated by Hyson et al. (1980). Hyson et al. do not give any analysis of the accuracy of their 'mismatched' diffusion scheme (see ii above) but it appears to be only accurate to first order. However, any errors that arise from this aspect are likely to be less serious than those arising from the use of upwind differencing of the advective transport. The higher order accuracy in the new model means that accurate results can be obtained with low resolution. A number of the calculations presented in subsequent sections were performed using both 10 and 20 zones and the differences were found to be very small.

v) The new model uses a spectral representation of the time variation and so the transport coefficients can be made to vary more smoothly than in the old model.

vi) The new model is implemented in a more modular fashion than the old model. This makes it possible to use it in a more flexible manner. The most striking example of this is the use of the new model in the 'source-deduction' mode described in Section 2.3 above. Enting (1984) gives an example of how using a well-structured Pascal/Algol like language, only 6 statements need to be added to convert a conventional numerical integration procedure into a procedure for carrying out the source deduction calculations. The new model is actually implemented in Fortran-77. In spite of the limitations of this language, implementing a source deduction routine still consists of making only minor changes to a numerical integration routine.

## 4 Modelling Distributions of $CCl_3F$

The distribution of $CCl_3F$ is studied as a test of the interhemispheric transport in the model. Figure 4 shows the distribution of sources in space and time as used in the modelling studies. The primary source of information on halocarbon sources is the Chemical Manufacturers Association (CMA, 1982). The total global release is shown for 1950 to 1982 on Figure 4b. The CMA data give the division between hemispheres as approximately 4% southern hemisphere sources and 96% northern hemisphere sources. Within each hemisphere we have followed Hyson et al. (1980) in assuming the distribution of releases is the same as for fossil fuel use. (see Rotty, 1983). Figure 4a represents the spatial release pattern as a cumulative distribution of release from south to north. This form of distribution can be applied to defining the relative source strengths in each zone for any grid spacing by taking differences at appropriate intervals. A

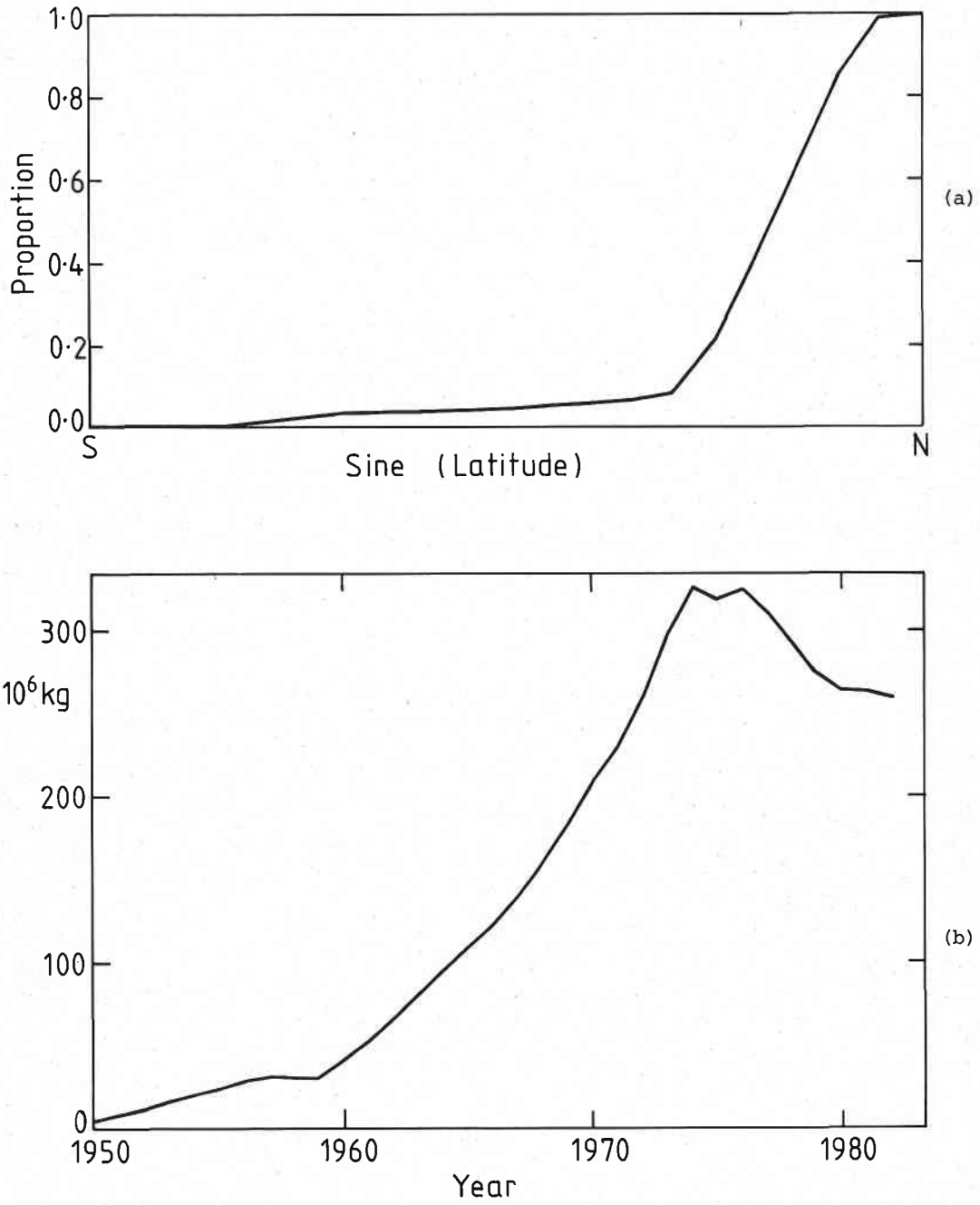


Fig 4: Description of $CCl_3F$ release in model. (a) Cumulative distribution of release with latitude. (b) Global total release rate as a function of time.

number of special studies were performed with 8% of the release in the southern hemisphere, to correspond directly to fossil fuel use. Because of the linearity of the model, the intermediate case of 6% southern hemisphere release (as estimated by Hyson et al., 1980, on the basis of aerosol usage) can be obtained by averaging the 4% case and the 8% case.

The observations that were used as the basis of comparison are 1980 annual means from the ALE program (Cunnold et al., 1983), multiplied by a factor 0.96 which represents the best current estimate of the correction required to convert the ALE scale to an absolute scale (Rasmussen and Lovelock, 1983).

The studies of $CCl_3F$ were undertaken to test the interhemispheric transport. However, in the course of these studies a major weakness of the transport coefficients was revealed in that the transport between the stratosphere and the troposphere was found to be too large. If a realistic stratospheric sink was included then the rapid transport into the tropical stratosphere led to too short an atmospheric lifetime and too large an interhemispheric gradient. Because of these difficulties, the studies presented here are for the case with no stratospheric sink. The results are comparable to observations of $CCl_3F$ only to the extent that a lifetime of 60 to 90 years can be regarded as infinite. This is a reasonable approximation when considering interhemispheric gradients but is less suitable for comparing total inventories. This means that when comparing the calculated distribution to the observations, the absolute values are of no special significance; it is the relative changes that should be compared. The calculated concentrations are actually those of the lowest layer; they have not been extrapolated to the surface. In order to bring the observations and the calculations into a single convenient range, the observations plotted in Figures 5 and 6 are annual means for 1980 while the calculated curves are for 30 June and 31 December, 1979. The extent to which the increase over 6 months is not spatially uniform gives an indication of the amount of spatial variation in the seasonal cycle produced by the model.

Figure 5 compares the observations against model calculations using the transport fields derived from the GCM/tracer model. The dashed curves were calculated using 10 zones and 10 equal height layers (each 0.4 scale heights) with 4% of the release in the southern hemisphere. The dotted curves were obtained using the same resolution, but with 8% of the release in the southern hemisphere. The solid curves on Figure 5 give the results of using 10 zones and 15 equal height layers (up to 4 scale heights) with 4% of the release in the southern hemisphere. The differences in the absolute concentration associated with changing the vertical resolution are mainly due to unrealistic small scale features in the preliminary transport fields. When improved transport fields are used, the resolution dependence is greatly reduced. In some preliminary calculations an even stronger dependence on the vertical resolution was obtained when the bound $K_{zz} \geq 5\ m^2 s^{-1}$ was not used. The omission of this constraint, which simulates the effect of small scale processes, allowed the occurrence of large concentrations in a shallow surface layer during summer and so induced a strong seasonal signal at high latitudes in disagreement with the observations (Harris and Bodhaine, 1983, their Figure 17). Calculations using 20 zones led to results very similar to those shown, confirming that, because of the second-order differencing scheme, there is little resolution dependence in the horizontal direction.

Figure 6 compares the observations to calculations using transport fields based on those tabulated by Hyson et al. (1980). The dashed curve shows the results of using these coefficients directly in the new model. It

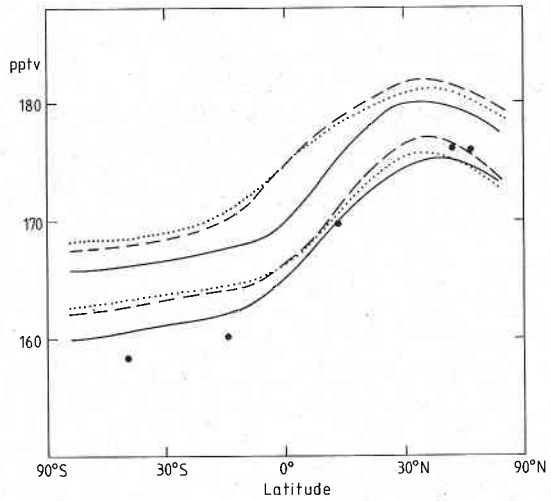


Fig 5: Interhemispheric gradient of $CCl_3F$, calculated using transport fields from the GCM. Pairs of curves are for 30 June 1979 (lower curves) and 31 December 1979 (upper curves). Solid curves calculated using 15 equal height layers and 10 zones with 4% of release in southern hemisphere. Dashed curve is 10 layers and 10 zones with 4% of release in southern hemisphere. Dotted curves are 10 layers and 10 zones with 8% of release in southern hemisphere. Points are 1980 means from the ALE program.

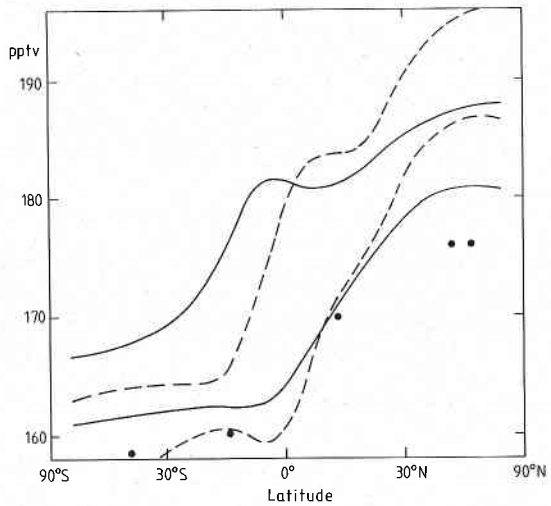


Fig 6: Interhemispheric gradient of $CCl_3F$ calculated using Eulerian mean circulations. Pairs of curves are for 30 June 1979 and 31 December 1979. Dashed curves calculated using diffusion coefficients based on those tabulated by Hyson et al. (1980). Solid curves calculated with horizontal diffusion doubled to compensate for the absence of the numerical diffusion that is present in the old model. Both calculations have 8% of release in the southern hemisphere and use 10 zones. Points are 1980 means from the ALE program.

is obvious that the interhemispheric gradient is far too large. This is in spite of the fact that the calculations using the transport fields from Hyson et al. were performed with 8% of the release in the southern hemisphere in order to try to reduce the gradient. The discrepancy occurs because the new model does not include the numerical diffusion implicit in the old model due to the use of first order upwind differencing. As an approximation, based on the mean value of the numerical diffusion, the horizontal diffusion coefficients used by Hyson et al. were doubled. The resulting interhemispheric gradient is shown as the solid curve on Figure 6. The agreement with observations is greatly improved. This sensitivity of the gradients to the diffusion coefficients contradicts the statements by Hyson et al. (1980) (see also Pearman et al.1983) that the transports are determined primarily by the advection and are relatively insensitive to the horizontal diffusion coefficients. This disagreement is because the adjustments performed by Hyson et al. (1980) never changed the 'numerical diffusion' and so the proportional changes that they made to the total diffusion were about 50% smaller than the proportional changes to their tabulated diffusion coefficients - hence the small effects on the interhemispheric gradients.

Thus the transport coefficients given by Hyson et al. (1980) are highly specific to their model and cannot be expected to be applicable to other differencing schemes or other grid spacings. Conversely, general sets of transport fields, such as the GCM-based fields used here, that are good approximations to the fields applying to the continuum limit will be unsuitable for use in the model of Hyson et al. In contrast, the use of a differencing scheme that is accurate to second order makes it possible to use the present model with a range of grid spacings without having to re-tune the transport coefficients.

## 5 The Seasonal Variation of $CO_2$

The seasonal variation of $CO_2$ was modelled as a further test of the new transport fields. Because the seasonally varying sources of $CO_2$ are poorly known the observations of surface concentrations of $CO_2$ were used to determine these sources and the model was validated using high altitude data.

The first step in determining the sources was to construct a smoothed representation of the variation of surface $CO_2$ concentration in space and time. The function that was used was

$$c(x,t) = c_0 + 1.5t + a_0(x) + a_1(x)\cos(2\pi t) + a_2(x)\sin(2\pi t) + a_3(x)\cos(4\pi t) + a_4(x)\sin(4\pi t) \qquad (5.1)$$

where $x = 0.5(1+\text{sine(latitude)})$ . (5.2)

The coefficients $a_n(x)$ were expanded as

$$a_n(x) = \sum_{m=0}^{J} b_{nm}\cos(m\pi x) \quad . \qquad (5.3)$$

Table 2 Coefficients describing space-time variation of $CO_2$ according to equation 5.

| | 1 | cos(2πt) | sin(2πt) | cos(4πt) | sin(4πt) |
|---|---|---|---|---|---|
| 1 | | .334 | 1.810 | .107 | -.636 |
| cos(πx) | -1.490 | -.865 | -3.054 | -.220 | 1.058 |
| cos(2πx) | -.294 | .850 | .819 | .415 | -.553 |
| cos(3πx) | .134 | -.264 | -.148 | -.401 | .085 |
| cos(4πx) | .338 | | | | |
| cos(5πx) | -.115 | | | | |

Table 3 Stations used to define spatial variation of seasonal cycle of $CO_2$.

| Site | No. months | Scale | x | Reference |
|---|---|---|---|---|
| Cape Grim Tas. | 69 | 81 | .174 | Beardsmore et al.(1984) |
| Macquarie Is. | 35 | 81 | .093 | " |
| Mawson | 52 | 81 | .038 | " |
| Sable Is. | 61 | 74 | .847 | Wong & Pettit (1981) |
| W. Ship P | 84 | 74 | .883 | " |
| Alert | 65 | 74 | .996 | " |
| Nth Pacific | 25 | 74 | .825 | Wong et al. (1981) |
| Barrow | 113 | 81 | .974 | Harris & Bodhaine (1983) |
| Samoa | 72 | 81 | .377 | " |
| South Pole | 84 | 81 | .000 | " |
| Fanning Is. | 49 | 81 | .534 | Mook et al. (1983) |
| South Pole | 191 | 74 | .000 | Bacastow & Keeling (1981) |
| Baring Head | 51 | 74 | .172 | Lowe et al.(1979) |

The various coefficients in the double expansion are given in Table 2. The interhemispheric gradient term $a_0(x)$ was expanded to order J = 5 by fitting the annual means obtained from GMCC surface sites (see Table 8 of Harris and Bodhaine, 1983). The other coefficients $a_n(x)$ were expanded to order J = 3 by fitting the composite data set listed in Table 3. This composite data set is not suitable for determining interhemispheric gradients because of the different calibration scales involved. In general, the data for each site were fitted by a constant plus terms in t, $t^2$, cos(2πt), sin(2πt), cos(4πt) and sin(4πt) at each site. For shorter records (<52 data points) the $t^2$ term was omitted. The corresponding coefficients describing the cyclic variation for each site were then fitted by a least squares fit to the form (5.3). The seasonal contribution to c(x,t) i.e., the part without the $a_0(x)$, the mean $c_0$ and the 1.5t trend, is plotted in Figure 7. Even though very few of the GMCC data were available for constructing this fit, the contours are generally similar to those obtained from the GMCC flask program (Harris and Bodhaine, 1983; their Figure 9).

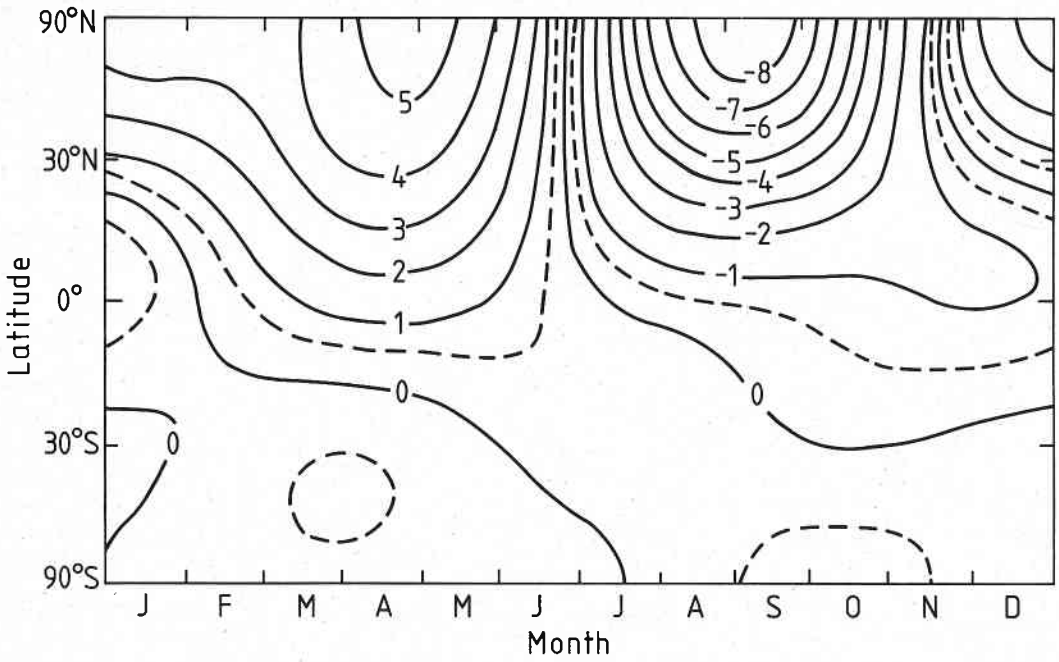


Fig 7: Contours of seasonal variation of $CO_2$ concentration from the function defined by Equations (5.1) and (5.2) with coefficients from Table 2, excluding mean interhemispheric gradient and secular trend.

The composite expression was then used to determine the surface sources of $CO_2$. The approach used here differs from the approach used by Pearman and Hyson (1980) in deducing biospheric $CO_2$ sources (see also Pearman and Hyson 1986). The main differences are

i) Total net sources (i.e. biosphere + oceans + fossil fuel) are deduced.
ii) A direct computational technique is used (see Enting, 1984) rather than the iterative approach used by Pearman and Hyson.
iii) The present study includes a preliminary error analysis. The uncertainties in the sources due to uncertainties in both the observed concentrations and in the model's transport fields are discussed.

The techniques for directly determining the sources are described by Enting (1984). Enting's analysis also uses Green's function formalisms to demonstrate that the problem of determining surface sources from surface concentration observations will formally have a unique solution. In practice this unique solution is rather poorly determined by the observations because it is ultimately the rates of change of concentration that determine the sources.

The numerical technique consists of simply performing a stepwise time integration to determine the concentrations at grid points above the surface. The transport model requires values of the concentrations at the previous time step (or for the predicted value at the current time point). For the surface sites these concentrations are obtained from expression (5.1)

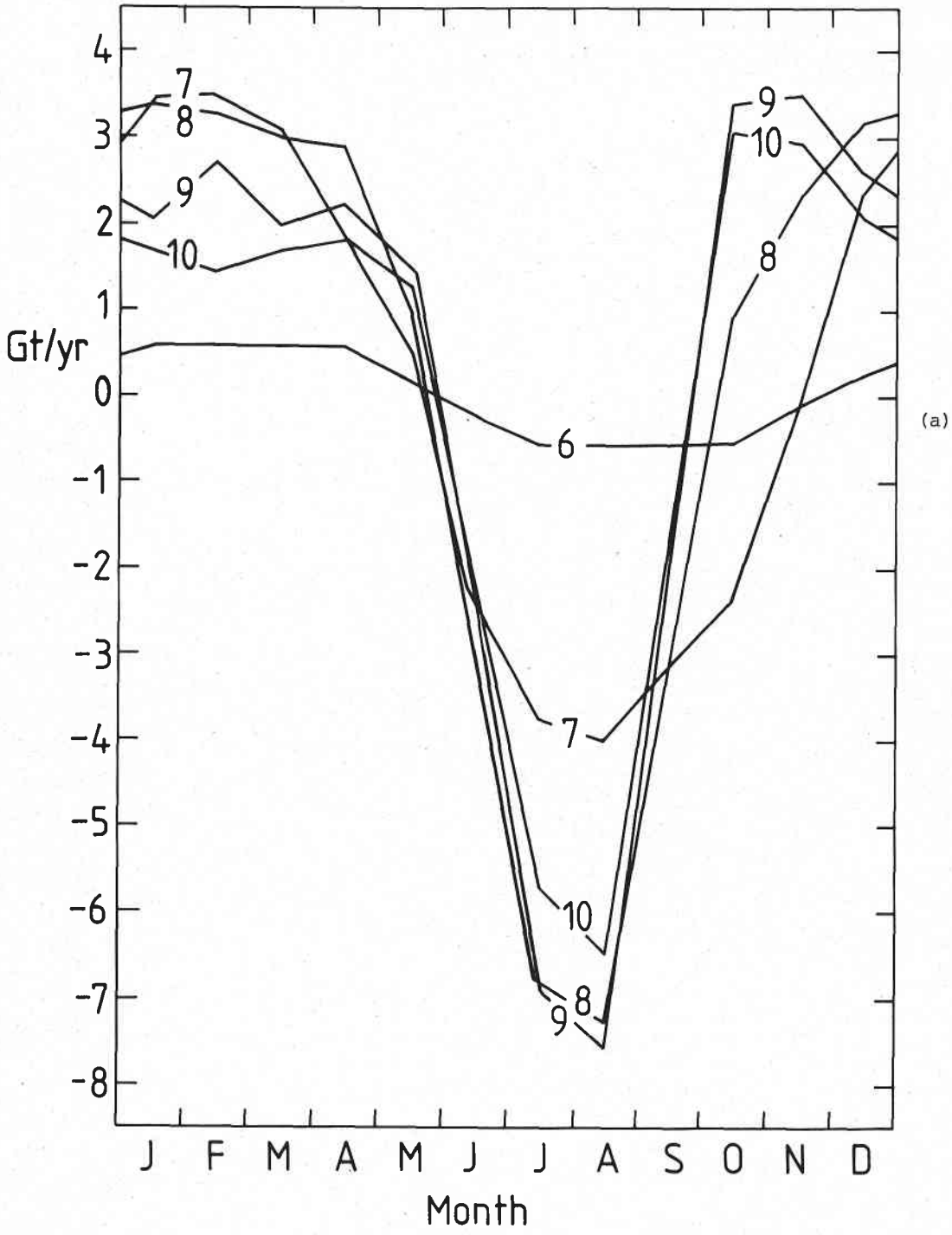


(a)

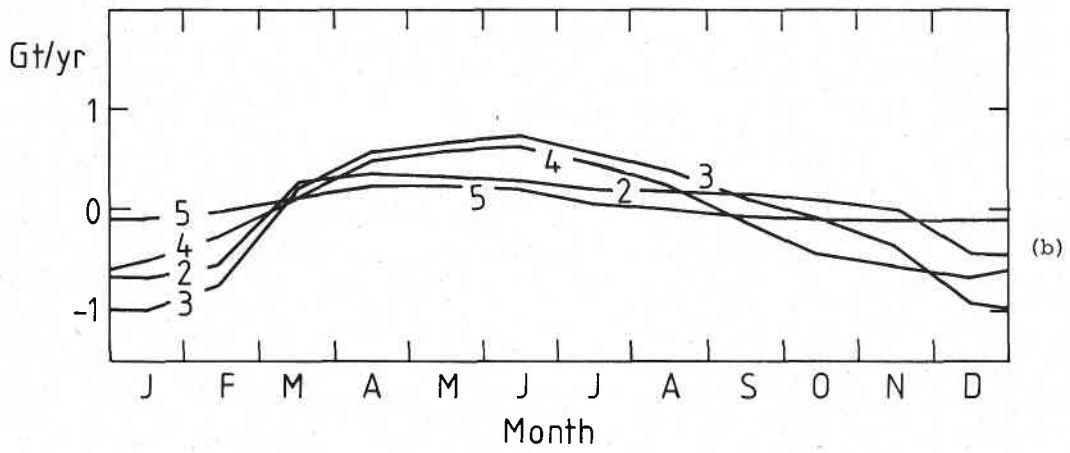


Fig 8: Biospheric source strengths for 10 equal area zones as given by Pearman and Hyson (1980) in gigatons of carbon per year, (a) northern hemisphere, (b) southern hemisphere. The Antarctic regions (zone 1) are assured to have no biospheric sources.

and the concentrations at the other grid points are generated at successive times by the numerical integration scheme. At each time step, Equation (3.5) is applied at all surface sites to determine the surface source strength. The transport model routines are used to evaluate the transport terms in Equation (3.5). The time integration is started using a uniform $CO_2$ distribution. The procedure converges rapidly and a steady periodic source distribution is achieved after 2 or 3 cycles. The surface $CO_2$ concentration is matched to the concentrations in the centres of the model cells at the lower boundary. It is not appropriate to perform any extrapolation to the surface because the bottom few kilometres of the atmosphere are well-mixed over the time scale for which the 2-d model is applicable.

The main results of these calculations are described in the following figures which give source strengths deduced for various cases. For comparison, Figure 8 shows the biospheric source strengths given by Pearman and Hyson (1980) grouped into 10 equal area zones. Figure 9 shows the total source strengths deduced using the techniques described above with Eulerian mean stream functions and the diffusion coefficients from Hyson et al. (1980) and the $K_{yy}$'s multiplied by 2 as described in Section 4. Figure 10 shows the source strengths deduced using the transport coefficients from the GCM/tracer model. For each set of transport coefficients, the calculations were performed using the model with 8 equal pressure layers and 10 equal area zones. While the source strengths are generally similar in the northern hemisphere, there are significant differences in the southern hemisphere. Relative to the case calculated using Eulerian stream functions, the sources deduced using the GCM results have an additional component representing a net transport of carbon from low to high lattitudes in the southern hemisphere of several gigatons per year. It should be noted that the source deduction problem is relatively ill-conditioned (Enting, 1985b) in that small-scale details will be swamped by errors in both the concentrations and the model.

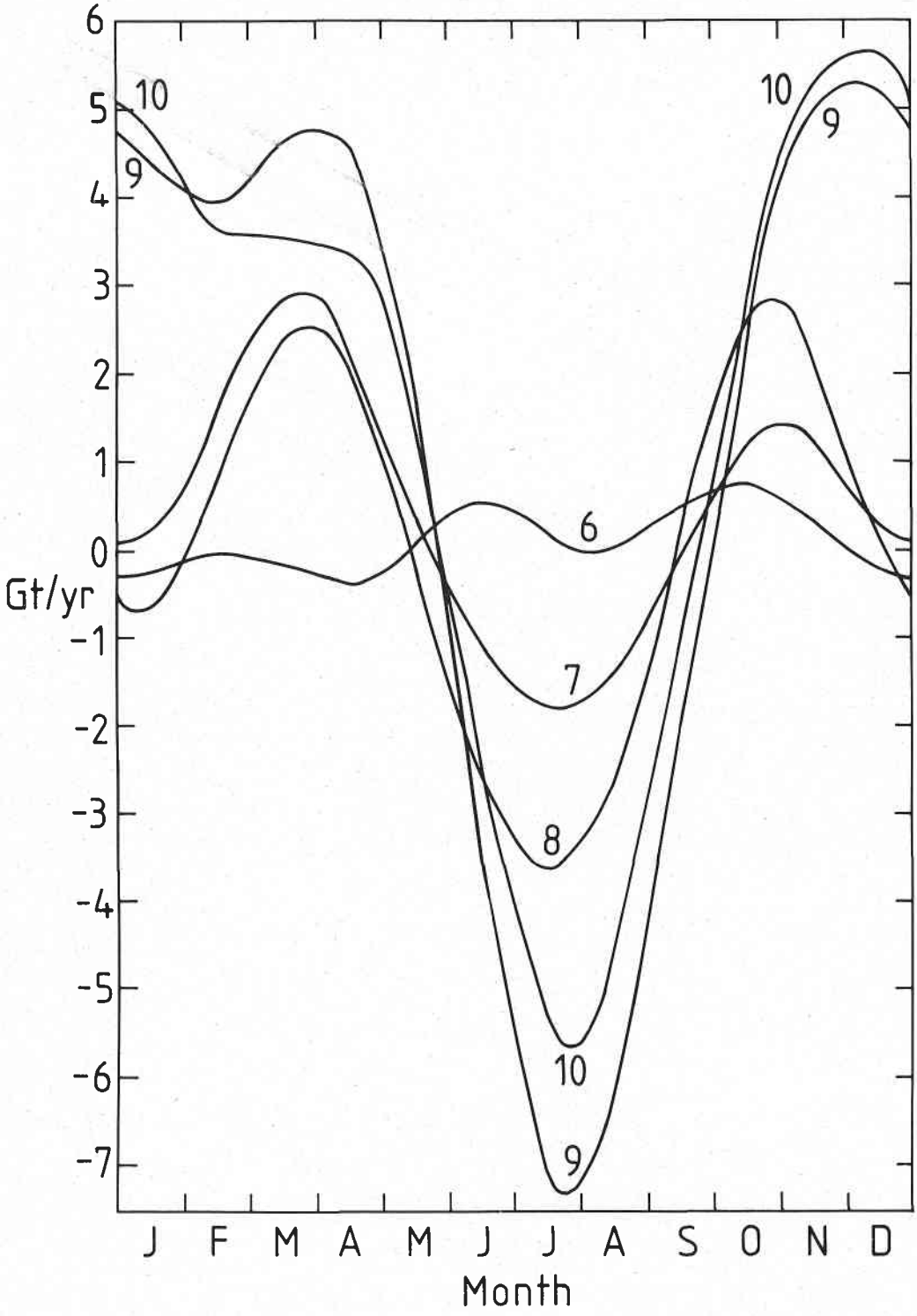


(a)

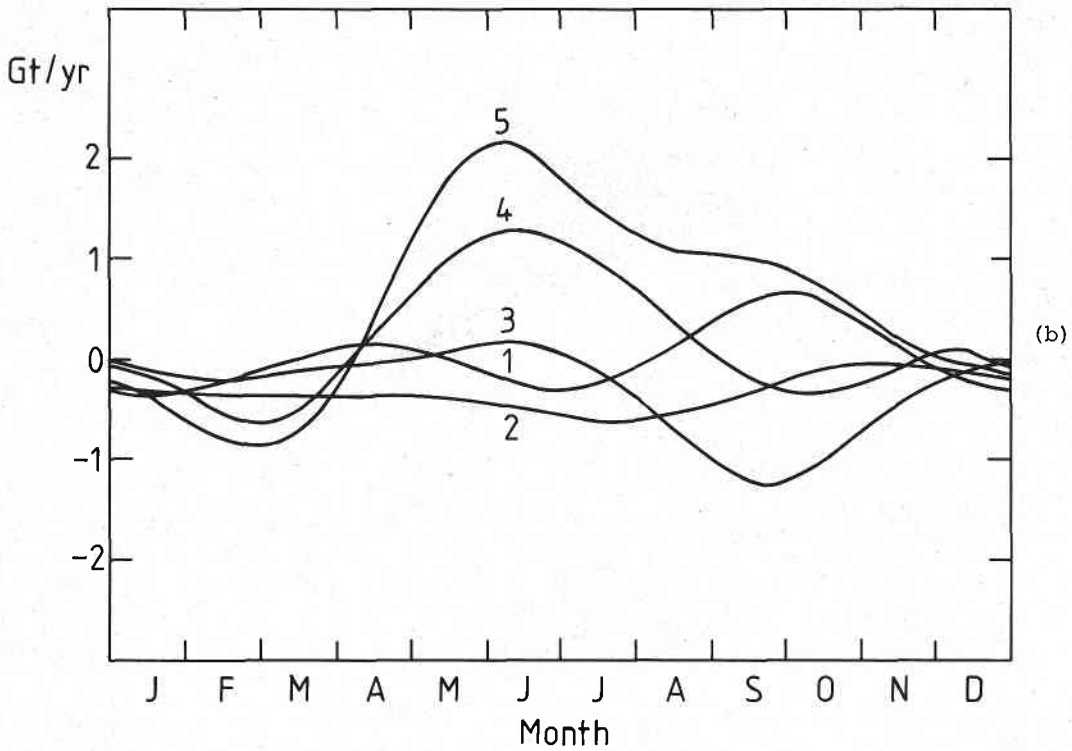


Fig 9: Plots of net source strength in gigatons carbon per year for 10 equal area zones 1 (southernmost) to 10 (northernmost) calculated using surface concentrations with coefficients from Table 2 in Equation (5.1) and using Eulerian mean circulations in the model. (a) northern hemisphere sources. (b) southern hemisphere sources.

While the major contributions to the northern hemisphere sources were similar with each set of transport fields and similar to the biospheric sources deduced by Pearman and Hyson (1980) some initial calculations using the GCM based transport fields without the constraint $K_{zz} > 5m^2/sec$ implied source distributions that were more highly localised in mid-latitudes of the northern hemisphere. This result underscores the importance of the small-scale vertical transports. Fung (1985) has pointed out that the GISS GCM treats such transports in a highly simplified manner. This may be the reason for the vertical attenuation of the seasonal signal in Fung's study being smaller than is observed and, as discussed by Enting and Pearman (1986), being consistent with much stronger biospheric sources than those deduced by Pearman and Hyson (1980). This point is discussed further by Pearman and Hyson (1986).

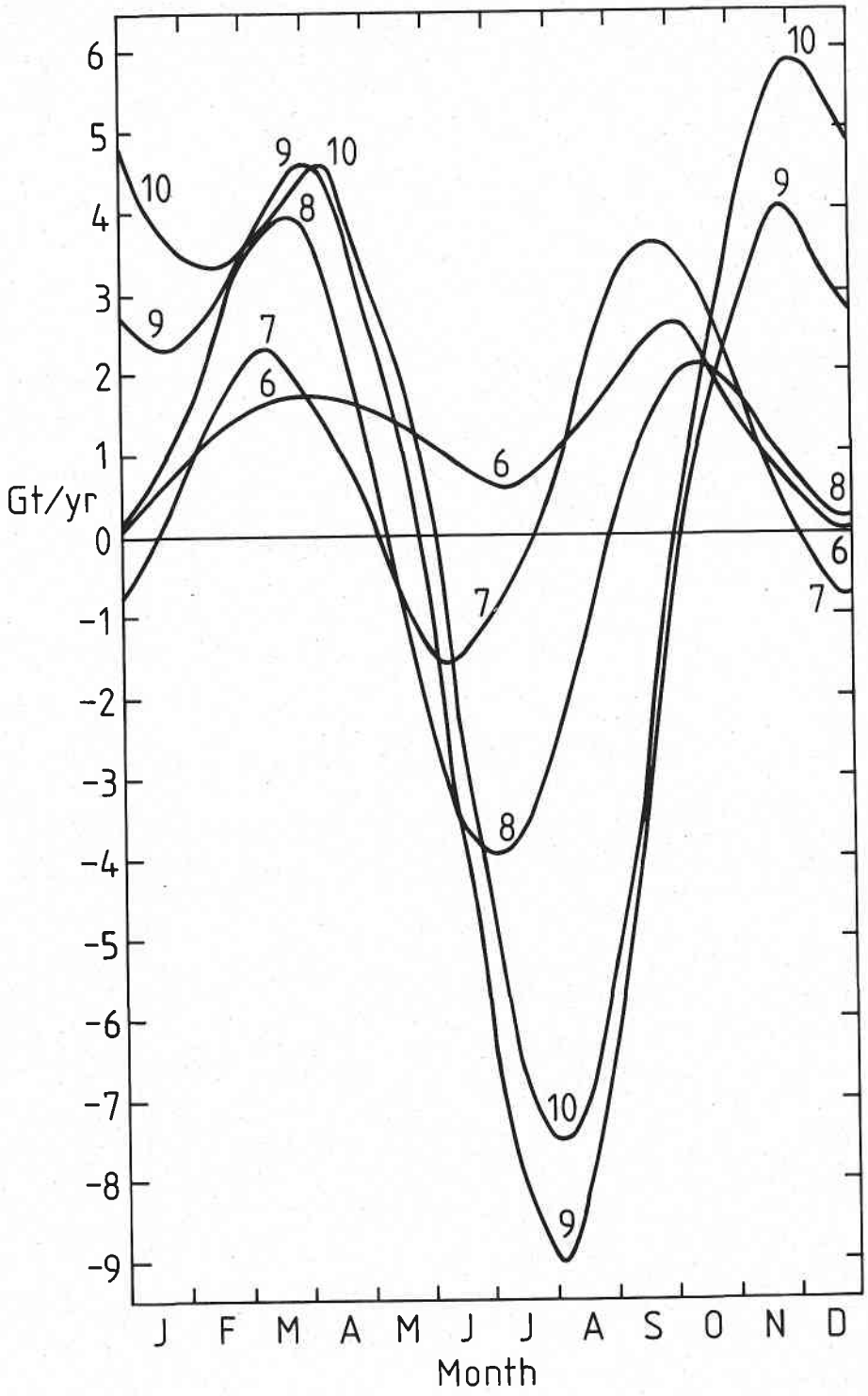


(a)

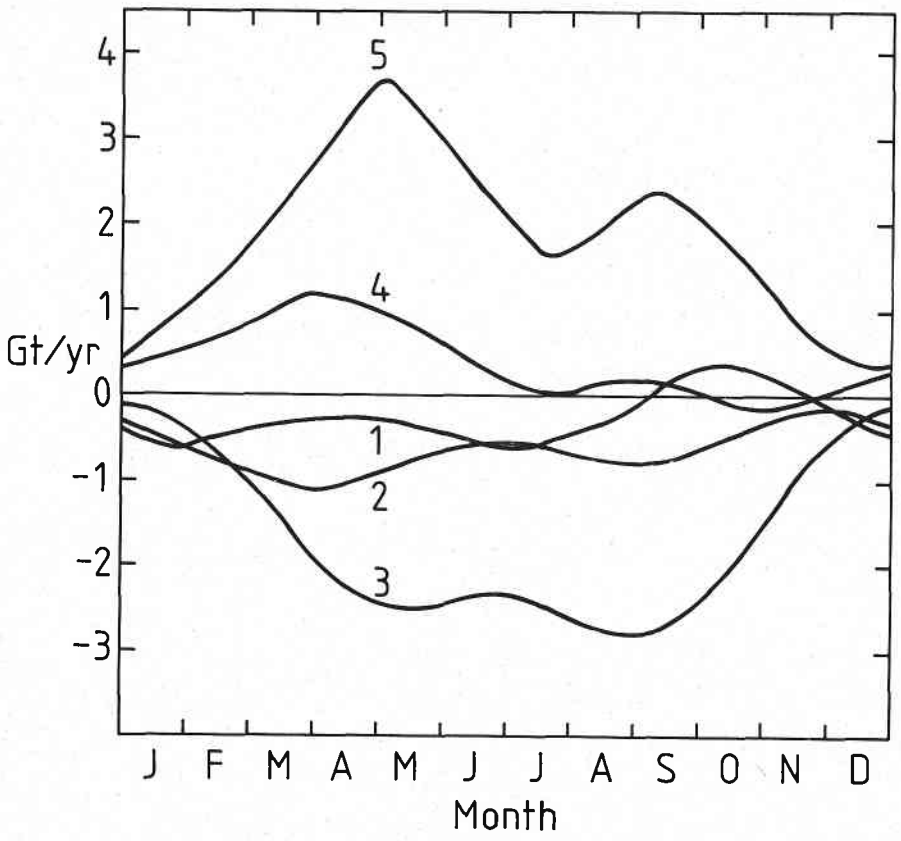


(b)

Fig 10: As for Figure 9 but calculated using transport fields from the GCM/tracer model.

The 'validation' tests are shown in Figures 11, 12 and 13 which compare the model calculations with observations in the mid-latitude southern hemisphere, the mid-latitude northern hemisphere and the tropics respectively. In each case the model results refer to the same two cases that were considered above: firstly the case with the transport coefficients from the GCM/tracer model, plotted as dashed curves, and secondly with the transport coefficients derived from those given by Hyson et al. (1980) with the $K_{yy}$ field doubled, plotted as dotted curves. Figure 11 shows the southern hemisphere results for latitude 44S and levels of 438mb (upper curve of each pair) and 938mb (the surface cell). Equation (5.1) defines the lower boundary condition and so was the same for each of the calculations.

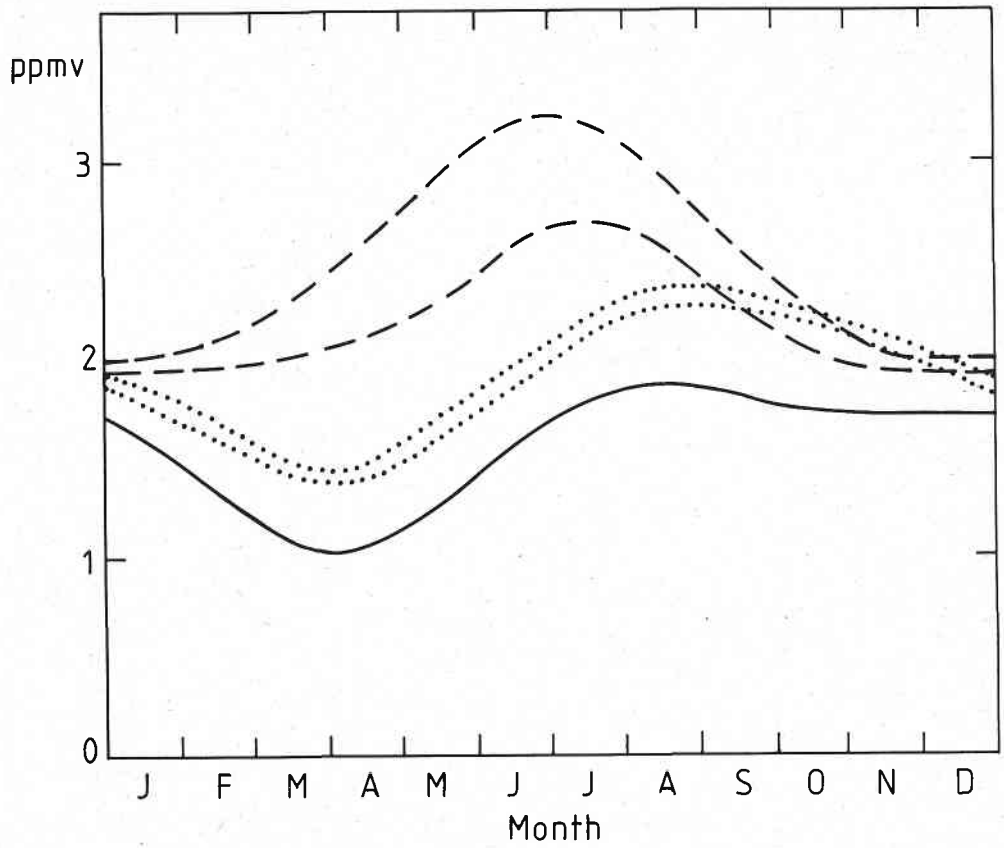


Fig 11: Seasonal cycle at high altitude in the southern hemisphere. Pairs of curves are for 438mb (upper curves) and 563mb (lower curves), all at latitude 44S. Dashed curves are calculated using transport fields from the GCM/tracer model. Dotted curves are calculated using transport fields with Eulerian mean stream functions. The solid curve is the surface concentration that was fitted.

The relevant data for comparisons are from the CSIRO aircraft sampling program (Pearman and Beardsmore, 1984). The model calculations do not represent the observed phase of the seasonal cycle particularly well. However the model results, particularly those using the GCM transport fields, do represent the observed amplitudes reasonably well and in particular they show how the amplitude increases with height. In addition, the model results reproduce the observed feature of having the peaks occur earlier as the height increases through the troposphere. Given this qualitative agreement, it is possible that the disagreement in the phases is due to the uncertainties in the phase of the surface variations since the seasonal cycle in the southern hemisphere is poorly determined and is subject to significant interannual variations (for further discussion see Thompson et al., 1986).

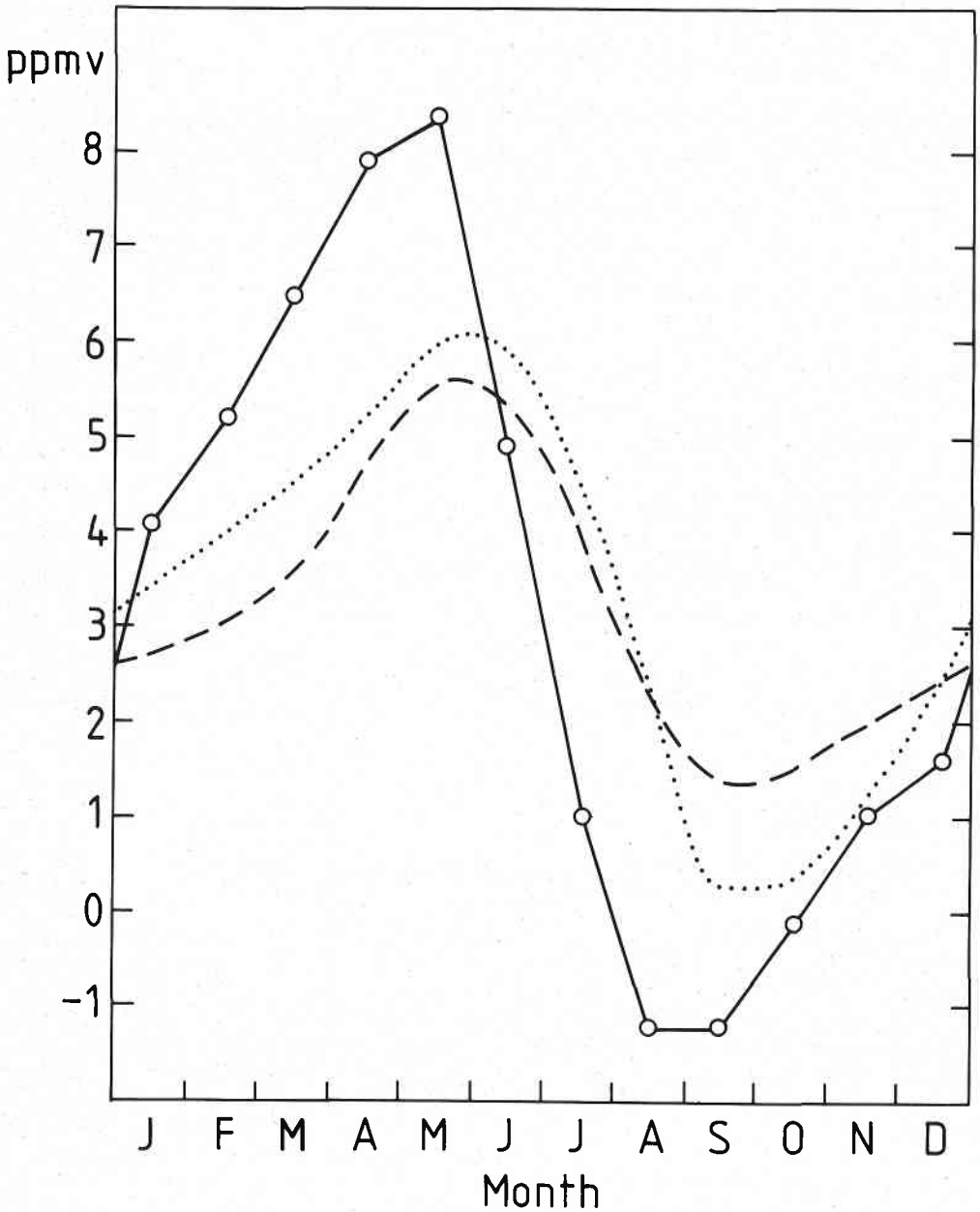


Fig 12: Seasonal cycle at high altitude in the northern hemisphere at 438mb and 44N. Dashed curve is calculated using transport fields from the GCM/tracer model. Dotted curve is calculated using transport fields with Eulerian mean stream functions. The circles connected by the solid line are detrended data for 5 to 6km from Tanaka et al. (1983).

Figure 12 shows the results for the northern hemisphere (44N at 438mb). The data shown on the figure are from Tanaka et al. (1983) with a trend of 1.5 ppmv/yr removed; the height is from 5 to 6 km. It will be seen that the model calculations give too small an amplitude in each case. Originally it was thought that this discrepancy may arise from the fact that, as described in Section 2, the present calculations do not include a complete representation of the small-scale diffusion processes. Subsequent tests with complete $K_{zz}$ fields have shown that the discrepancy remains.

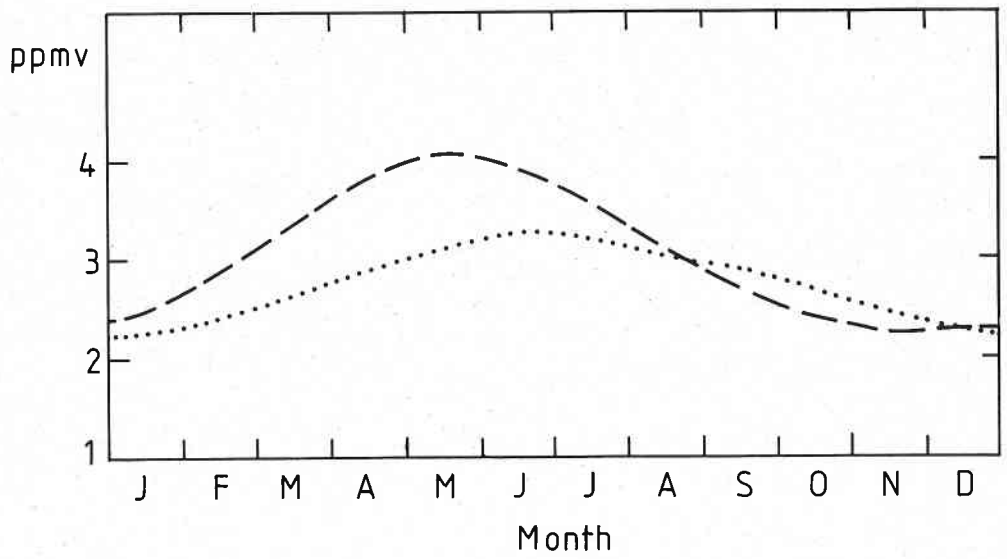


Fig 13: Seasonal cycle at high altitude in the tropics (6S) at 563mb. Dashed curve is calculated using transport fields from the GCM/tracer model. Dotted curve is calculated using transport fields with Eulerian mean stream functions.

Figure 13 shows the variations at 6S and 563mb. This location would correspond to the Cosmos station in the GMCC network. The relevant data have not been published in numerical form but are plotted in Figure 5 of Bodhaine and Harris (1982). While the observational record defines the seasonal cycle rather poorly, it appears that the observed cycle has a peak to peak amplitude of about 5 ppmv which is more than twice the value calculated using the GCM fields and 4 or 5 times the value calculated using the Eulerian mean calculations.

Finally, the uncertainties in the sources obtained by the techniques described here must be discussed. The most obvious indication of the possible uncertainties is given by a comparison of the sources deduced from the two different sets of transport coefficients. As mentioned above, the main differences occur in the southern hemisphere where for the same surface concentration values the different circulation patterns imply significant differences in the locations of the regions which act as net sources and sinks.

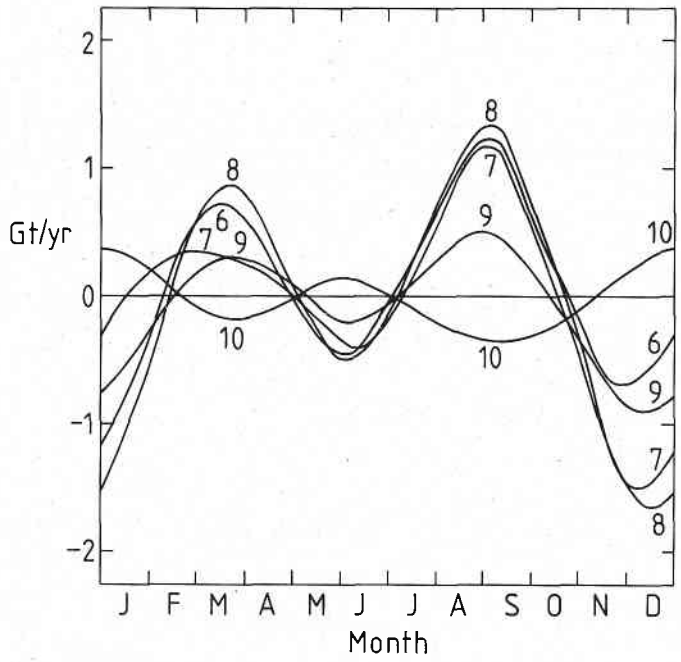


(a)

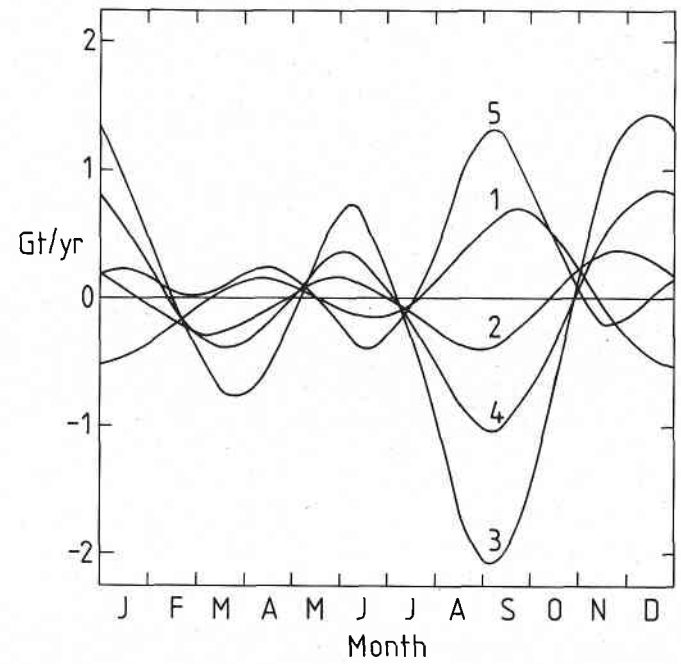


(b)

Fig 14: Changes in source strengths due to changing the truncations used in fitting the spatial variations as calculated using the transport fields from the GCM tracer model. (a) northern hemisphere (b) southern hemisphere.

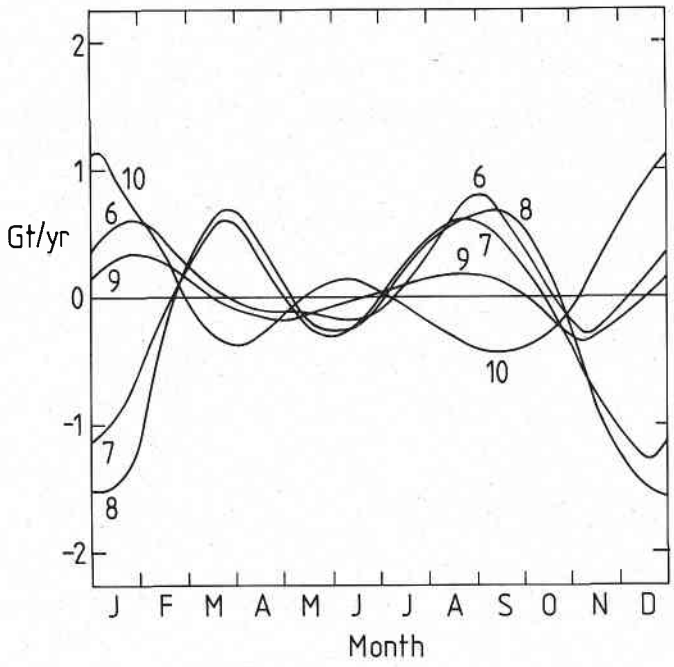


(a)

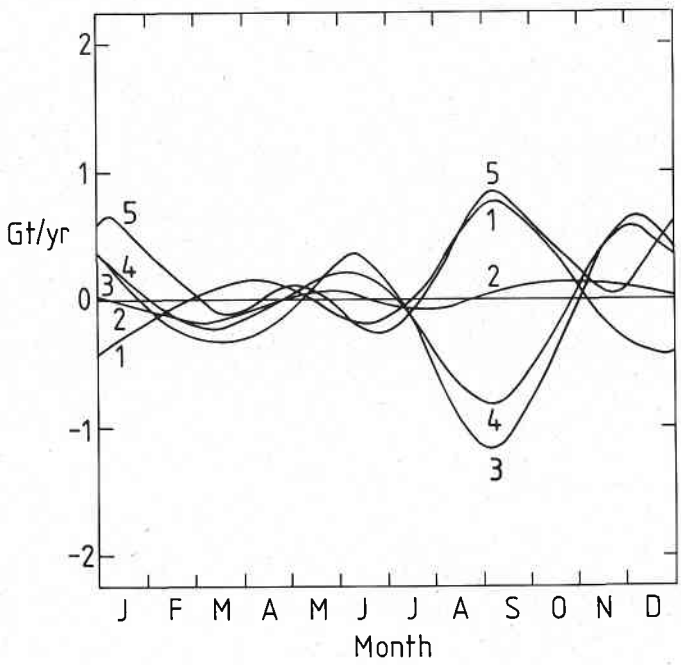


(b)

Fig 15: As for Figure 14 but calculated using Eulerian mean circulations.

The other contribution to the uncertainties in the sources is, of course, the uncertainties in the concentrations that are fitted. Because the source deduction calculations are linear, it follows that errors in the sources can be obtained by applying the source deduction procedure directly to estimates of the errors in the concentrations that are fitted. As an indication of the possible uncertainties, Figures 14 and 15 show the changes in source strengths in each zone associated with changing the order of the expansion of the seasonal variation. The differences in concentration are the differences obtained by changing the limit of the summation from $J = 3$ to $J = 2$ for $n > 0$ in Equation (5.3), i.e. we considered truncation errors in the function plotted in Figure 7 but no change was made to the interhemispheric gradient or the secular trend. Since the data are not obtained from uniformly spaced sites, changing J will lead to a change in all of the coefficients obtained by a least squares fit. An inspection of the curves shows that much of the uncertainty is associated with the distribution of the sources within each hemisphere at any particular time.

As noted above, the source-deduction problem is ill-conditioned in that the small-scale details of the sources are very sensitive to errors in both the model and the concentrations. This has been appreciated since the work of Bolin and Keeling (1963) who concluded that 'no details of the distribution of sources and sinks are reliable'. The conditioning of a model can be described by the behaviour of the error amplification as a function of the meridional wave number. The one-dimensional diffusion model used by Bolin and Keeling had the error amplification growing as the square of the wave number. As reported by Enting (1985b) the present model gives a linear growth in the error amplification as a function of meridional wave number. Subsequent tests using the transport fields from Hyson et al. (1980) show that a similar linear growth also occurs in that case. Although the ill-conditioning in the present model is not as severe as in the less realistic model of Bolin and Keeling, it still leads to serious problems, particularly when attempting to deduce southern hemisphere sources. In the southern hemisphere, the seasonal cycle is relatively poorly-determined and these uncertainties will be magnified by the source deduction process. One possibility for improving the reliability of estimates of surface sources is to perform some type of constrained inversion by using upper tropospheric data. A series of studies to determine the extent to which such data might stabilise the source-deduction problem is currently in progress.

## 6 Carbon-14 And Other Products Of Weapons Testing

The radioactive debris from the testing of nuclear weapons has often been used in the calibration of atmospheric transport models, particularly one-dimensional (height only) models. Such tracers would seem to be ideal for this purpose because in many ways the release pattern can be interpreted in terms of the mathematical idealisation of a 'point-source'. While the test programs of the USA and USSR spanned the period 1945 to 1962, each test series involved releases that were much greater than any previous series. Therefore at most times since 1950 the amount of any long-lived radioactive tracer in the atmosphere has been determined mainly by whichever of the major test series had occurred most recently.

Our attempts to model the behaviour of $^{14}C$ in the atmosphere have however encountered considerable difficulties. Some of these difficulties are to be expected because, like most other tracers, there are uncertainties in the atmospheric transports (which are our primary interest here), the sources (much of the information is classified as secret) and the biospheric and oceanic sinks (since the isotopic equilibriation will be determined by the gross carbon fluxes rather than the net fluxes involved in carbon cycle modelling). These difficulties have led to much confusion concerning the seasonal variations of $^{14}C$ during the period 1962-1967.

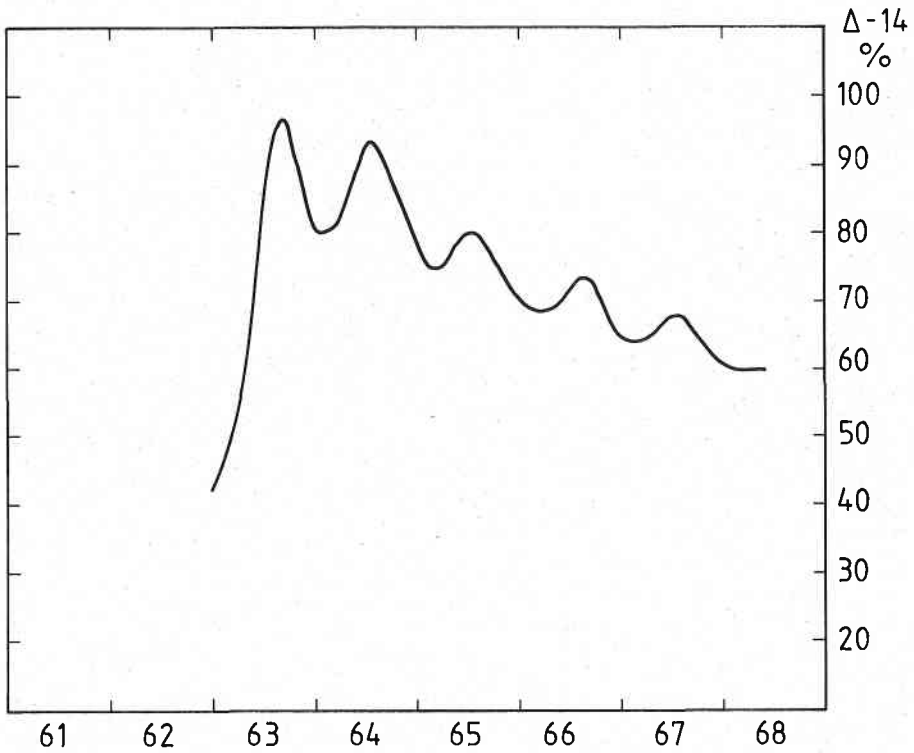


Fig 16: Variation in surface $^{14}C$ levels in the mid-to-high latitudes of the northern hemisphere, based on Nydal and Lovseth (1983).

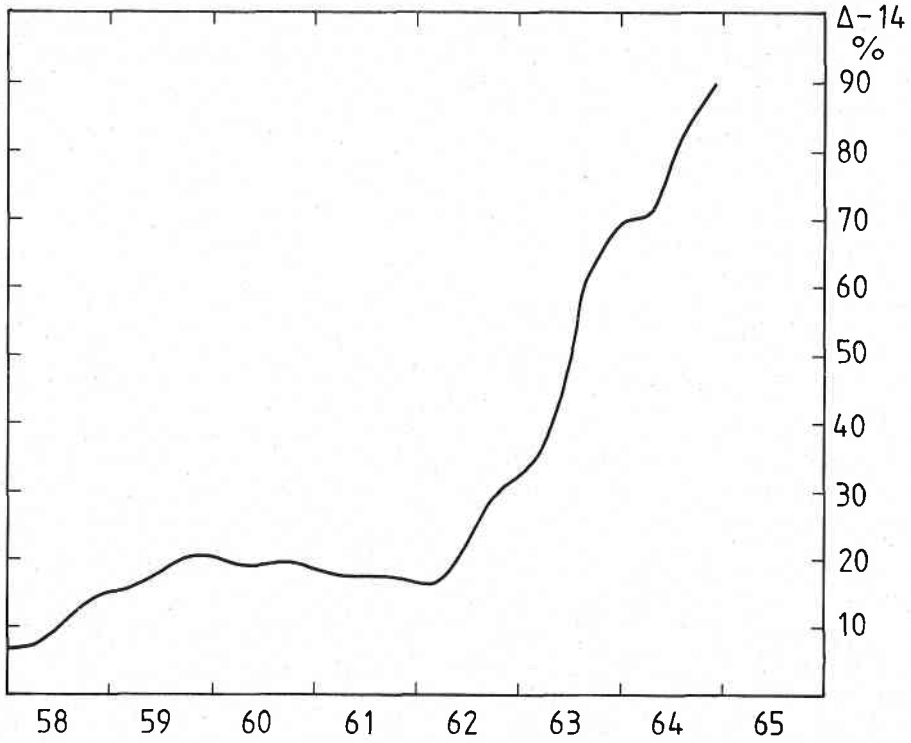


Fig 17: Variation in $^{14}C$ in the northern troposphere as calculated by Hyson (pers.comm., see also Pittock, 1983).

## 6.1 Difficulties with the Seasonal Variation of Carbon-14

The $^{14}C$ curve in Figure 16 is a representation of the observed variation of $^{14}C$, expressed as Δ-14‰, the deviation of the isotopic ratio from the standard ratio. It is based on samples collected at coastal sites (all on the west of the Atlantic) using 7-day collection periods (Nydal and Lovseth, 1983). The most striking feature of the curve is the seasonal variation which showed a peak in August 1963 and had peaks in July in subsequent years.

The main possible explanations for the seasonality are:

i) The seasonality reflects the seasonality of the stratospheric injection.
ii) The seasonality reflects the stratospheric injection, modified by the fact that $^{14}C$ is not "rained out" like other radioactive tracers and so continues to accumulate even when the net injection rate is falling.
iii) The seasonality reflects the combination of seasonal injection as described above with the amount of accumulation modulated by strong seasonal variations in the rate of loss of $^{14}C$ to the southern hemisphere.

iv) The surface variations observed by Nydal and others simply do not represent the behaviour of the bulk of the troposphere and that above the surface the seasonal behaviour is quite different to that shown in Figure 16.
v) The $^{14}C$ signal is due to local sources and so the signal observed by Nydal and Lovseth is not zonally representative.
vi) The seasonal variation is due to seasonal variations in the rate of uptake of $^{14}C$ by the oceans.
vii) The seasonality is due to biospheric effects.
viii) The seasonality is due to contamination effects from fossil fuel $CO_2$.

## 6.2 Seasonal Influences On Carbon-14 From Atmospheric Transport

The first four of the eight possible explanations of the seasonal variation of $^{14}C$ involve the details of the zonally averaged atmospheric transports. The other explanations invoke effects that require the modelling of additional processes. These other possibilities are discussed qualitatively in Section 6.3 below.

Firstly, in connection with explanation (v) above, it must be noted that surface data from Barrow (Young and Fairhall, 1968) and Central Europe (Munnich and Vogel, 1963) confirm the seasonal cycle described by Nydal and Lovseth. It should also be noted that the seasonal variations of most other radioactive tracers (e.g. $^{90}Sr$ and $^{3}H$) show peaks in the northern spring compared to the summer peaks of $^{14}C$. A large number of data sets for such tracers are reviewed by Reiter (1978).

Figure 17 shows the results of a preliminary modelling study of the distribution of $^{14}C$ in the atmosphere. These results were obtained by Hyson (personal communication) using the 'old' two-dimensional model. The ocean sink uses the formalism described by Pearman et al. (1983) to determine seasonally varying gross fluxes of $CO_2$. The isotopic fluxes are determined by taking the isotopic ratios of the source reservoirs and applying appropriate fractionation factors. A similar approach is used for the biospheric exchange, but a rather crude representation was used for the gross fluxes. These were represented by a rescaling of the net fluxes. A refined biospheric model for use in isotopic studies is described by Pearman and Hyson (1986). The input of $^{14}C$ was based on estimates of nuclear test yields assembled by Enting (1982) and using a conversion factor of $2 \times 10^{26}$ atoms per megaton. A brief account of the calculation with some contour plots of the zonally averaged $^{14}C$ distribution has been given by Pittock (1983).

Comparing the calculations shown in Figure 17 to the observations shown in Figure 16 it will be seen that the initial rate of increase is too small and the seasonal variation is virtually absent. There are two possible reasons for the slow rate of increase. Firstly because heights were based on cumulated yields the model calculations tended to inject the $^{14}C$ at a higher altitude than that given by Peterson (1970). Secondly, and probably more importantly, the slow rate of increase is due to the limited accuracy of the assumption, used by Pearman et al. in the old model, that the Eulerian mean circulation in the stratosphere is exactly cancelled by the off-diagonal part of the diffusion tensor.

Calculations performed using the new model with the transport fields derived from the GCM/tracer model have also failed to reproduce the seasonal variation shown by $^{14}C$. In order to perform a systematic investigation on the way in which the model distributes the products of

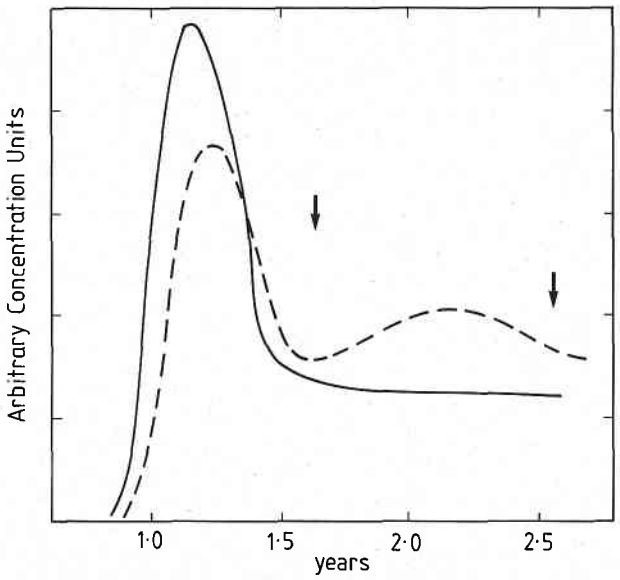


(a)

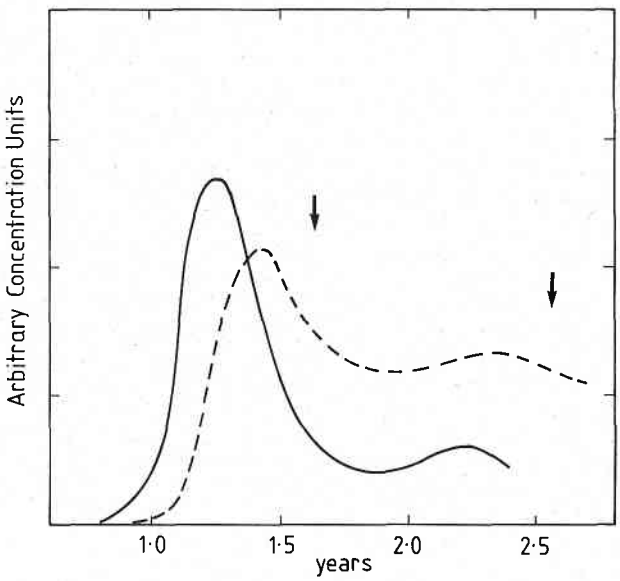


(b)

Fig 18: Variations in surface concentrations from single sources in October of year 1, using transport fields from the GCM/tracer model. The origin is January 1 of year 1. The arrows show the times at which peaks would be expected on the basis of Nydal's data. (a) Equal height calculations using 20 layers up to 5 scale heights with injection over range 1.9 to 3.8 scale heights (solid curve) and 2.7 to 5.3 scale heights (dashed curve). (b) Equal pressure calculations with injection into topmost of 30 layers. Atmospheric concentrations with no rainout (dashed curve), concentration of material removed by rainout (solid curve) with a residence time of 0.1 year below 300 mb.

nuclear testing, a series of calculations of the distributions from single point releases was undertaken. The time of release was in the (northern) fall of year 1 to correspond approximately with the peak releases of 1961 and 1962. The releases were at the latitudes of either Bikini (11N) or Novaya Zemlya (75N) and at various heights in the stratosphere.

The most important influence on the observed behaviour at the surface was found to be the height of release. Most of the tests were performed using the 'equal height' grid in order to obtain adequate resolution in the stratosphere. As an example, Figure 18a compares the calculated behaviour at the surface in the northernmost zone for a release between 1.9 and 3.8 scale heights (solid curve) and a release between 2.7 and 5.3 scale heights (dashed curve). It will be seen that for low releases the seasonality tends to disappear while for higher releases the peak is several months too early. The calculations seem to contradict explanation (i) above that attributes the seasonality directly to the seasonality of stratospheric injection. Since 'rainout' processes were not included in the calculations leading to Figure 18a while of course interhemispheric transports were included, the results shown are also in contradiction to explanations (ii) and (iii) above. It will be recalled that the calculations for $CCl_3F$ presented in Section 4 suggest that the GCM/tracer model fields give approximately the correct amount of interhemispheric transport. The inclusion of a 'rainout' effect seems to have relatively little influence on the timing of the peak. Figure 18b compares the northern hemisphere concentrations for a release at 29.5 km with no 'rainout' (dashed curve) and with a 'rainout' term that corresponds to a residence time of 0.1 year below 300 mb (solid curve). The reason for this lack of dependence on the rainout seems to be that so far as the northern hemisphere is concerned, losses through rainout serve simply as an alternative to losses through interhemispheric transport. This would seem to be particularly true in the three-dimensional calculation of Mahlman and Moxim (1978) where the 'rainout' was predominantly in the tropics. The comparison between the data and the direct two-dimensional calculations seems to preclude any of the first five explanations proposed above for the seasonal variation of $^{14}C$. The timing of the peaks is significantly different from the times expected on the basis of seasonal variations in vertical transport regardless of whether the transport variations are deduced from the GCM/tracer model or from observations of other radioactive tracers.

The present calculations support the conclusion by Karol (1970) that the spring fallout maximum of most tracers is due to maximum vertical transport in winter. The modelling studies would indicate that $^{14}C$ does not continue to build up in the northern hemisphere for much longer than other tracers - loss to the southern hemisphere caused $^{14}C$ to decline in a manner similar to the way in which other radionuclides decline due to rainout.

It should be noted that neither the calculations, nor low latitude observations (Nydal and Lovseth, 1983) support the suggestion of strong seasonal variations in the interhemispheric transport being a cause of the northern hemisphere variations.

The failure of the modelling calculations to obtain a consistent description of the seasonality is in agreement with two earlier studies. Munnich and Vogel (1963) used a one-dimensional diffusive model of the troposphere. They used tritium data to determine the seasonal variation of stratosphere to troposphere transport but could only reproduce the $^{14}C$ data

if they used very low values for the horizontal transport. Young and Fairhall (1968) estimated transports from wind data and adjusted the stratosphere to troposphere transports to fit the $^{14}C$ data. They obtained maximum injections late in spring in contrast to the winter maximum expected on the basis of other tracers and on dynamical consideration. Finally, it should be noted that if the seasonal cycles of the upper and lower troposphere were 6 months out of phase the resulting gradients would imply fluxes far in excess of what is possible given the amount of $^{14}C$ in the atmosphere. This would suggest that the upper tropospheric cycle discussed by Fishman et al. (1979) with peaks in January 1964 and April 1965, arises from the limitations of data that are both noisy and sparse.

## 6.3 Other Seasonal Effects

There are also considerable difficulties with the other mechanisms proposed in Section 6.1 as explanations of the seasonal variation of $^{14}C$. The suggestion that the seasonality described by Nydal and Lovseth is not zonally representative would seem to be inconsistent with the data. The high degree of coherence between different latitudes would seem to preclude any possibility of the seasonality being due simply to local sources. In addition, the observations from Barrow and Puget Sound (Young and Fairhall, 1968) or from Germany (Munnich and Vogel, 1963) give the same seasonal pattern with peaks in July.

The possibility of the seasonality being due to seasonal variations in ocean uptake was suggested by Young et al. (1965) on the grounds that the decrease in the (northern) fall must be due to the exchange of carbon into a reservoir of lower activity. Although this suggestion explains the phase of the signal, because the ocean uptake should be largest in winter, there are still a number of difficulties. In particular it would be expected that the amplitude of the seasonal signal would be proportional to the mean difference in $\Delta$-14 between the atmosphere and the ocean mixed layer. However the northern hemisphere signal decays more rapidly than would be predicted on this basis. Also, the seasonal signal in the southern hemisphere is smaller than would be expected, even without making allowance for the greater area of ocean. However, as mentioned above, a later study (Young and Fairhall, 1968) which did include a seasonal variation in ocean uptake, was only able to describe tropospheric $^{14}C$ variations by having the maximum injections occur late in spring. In addition, as will be seen from Figure 17, the preliminary modelling study by Hyson which also included a seasonally varying ocean uptake rate fails to give an appropriate seasonal $\Delta$-14 variation.

The last two possibilities mentioned in Section 6.1 were only included for completeness and can be readily dismissed as giving too small an effect to explain the seasonality. In principle there are two biospheric influences on the seasonal behaviour of $\Delta$-14. The first influence is simply a dilution effect due to the seasonally varying release of $CO_2$ from the biosphere. This $CO_2$ will be of relatively low $^{14}C$ activity in the period immediately following testing and so the dilution would lead to a maximum in the (northern) fall. However this cycle would amount to only about 2 to 3% signal in $\Delta$-14 compared to the 20% that is observed. The biosphere will also affect the $\Delta$-14 seasonality by being a seasonally varying sink of carbon. However, since the maximum uptake occurs in summer, the phase is the opposite of what is required.

The effect of 'contamination' by local sources of fossil fuel $CO_2$ has been discussed by Tans (1981) on the basis of his measurements in the

Netherlands. He estimated a contamination effect of 2% in summer and 4% in winter. Similarly, Munnich and Vogel (1983) found serious contamination effects at only a few sites in Europe. Thus in general the effect is far too small to give the observed seasonal changes even without allowing for the fact that sites such as Nordkapp (Nydal and Lovseth, 1983) will have much less contamination than inland sites in western Europe.

## 7 Conclusions

Preliminary transport fields obtained from the GCM/tracer model of Mahlman and Moxim (1978) have been used in two-dimensional modelling of the distribution of several tracers. In view of the fact that the transport fields have not been "tuned" in any way, the general agreement between the model calculations and observations of tracer distributions is remarkably good. There are however a number of anomalies that suggest that it may ultimately be necessary to tune the transport fields in some way. It must be emphasised that if the effective transport circulation is given by the small residual arising from the near-cancellation of the Eulerian mean circulation and the antisymmetric part of the diffusion tensor then it is to be expected that some aspects of the effective circulation may be poorly determined.

The studies of the distribution of products from nuclear testing suggest that the transport fields from the GCM give a reasonable description of some aspects of transport between the stratosphere and the troposphere. However, as discussed in Section 6, $^{14}C$ still appears anomalous and further work will be required to choose between the various conflicting explanations of the seasonal variation.

While it is possible that all of the anomalies noted in the studies presented in this paper could be due to uncertainties in the tracer sources and sinks or uncertainties in the observations, it seems more probable that at least some of the discrepancies are due to the transport formulation. Subsequent studies, to be reported elsewhere, have used a refined representation of the transport mechanism and revised values of the fields. These changes have led to improvements in transport between the stratosphere and troposphere. In addition, it may be necessary for the transport coefficients to be tuned in some way to improve the agreement between the modelling studies and the observations of tracer distributions. Such tuning represents a very complicated process because, in principle, it is necessary to consider a number of constituents simultaneously while also taking into account the uncertainties in the various sources. The most appropriate approach to this type of problem would seem to involve some form of constrained inversion employing one of the formalisms used in oceanography (see for example Wunsch, 1978, Wunsch and Minster, 1982), ocean chemistry (Bolin et al., 1983)., seismology (Wiggins, 1972, Pavlis and Booker, 1980) or carbon cycle modelling (Enting, 1985a, Enting and Pearman, 1986). Further discussion of such possibilities is outside the scope of this paper. The important point to note is that constrained inversion formalisms are helped considerably by having a good first approximation to the unknown fields. The studies presented in this paper would suggest that the transport fields derived from the GCM/tracer model give a good set of 'untuned' transport coefficients for use as a basis for any systematic refinement procedure.

References

Bacastow, R.B. and Keeling, C.D. 1981, Atmospheric carbon dioxide concentrations and the observed airborne fraction. pp103-112 of Carbon Cycle Modelling. SCOPE 16. ed. B.Bolin (John Wiley and Sons, Chichester).

Beardsmore, D.J., Pearman, G.I. and O'Brien, R. 1984, The CSIRO (Australia) Atmospheric Carbon Dioxide Monitoring Program: Surface Data. Division of Atmospheric Research Technical Paper No. 6 (CSIRO) 115 pp.

Bodhaine, B.A. and Harris, J.M. 1982, Geophysical Monitoring for Climatic Change. No. 10. Summary Report 1981. (U.S. Dept. Commerce) 158 pp.

Bolin, B, Björkström, A., Holmén, K. and Moore, B. 1983, The simultaneous use of tracers for ocean circulation studies. Tellus 35B 206-236.

Bolin, B. and Keeling, C.D. 1963, Large-scale atmospheric mixing as deduced from the seasonal and meridional variations of carbon dioxide. J. Geophys. Res. 68 3899-3920.

Brasseur, G. and Solomon, S. 1984, Aeronomy of the Middle Atmosphere. (Reidel, Dordrecht) 441 pp.

Clark, J.H.E. and Rogers, T.G. 1978, The transport of conservative trace gases by planetary waves. J. Atmos. Sci. 35 2232-2235.

Clough, S.A. 1980, Two dimensional chemical modelling in the U.K. Meteorological Office. Presented at the WMO workshop on two-dimensional models. Toronto, Feb. 1980.

CMA 1982, World Production and Release of Chlorofluorocarbons 11 and 12 through 1980. Chemical Manufacturers Association Fluorocarbon Program Panel. September 15, 1982.

Cunnold, D.M., Prinn, R.G. Rasmussen, R.A., Simmonds, P.G., Alyea, F.N., Cardelino, C.A., Crawford, A.J., Fraser, P.J. and Rosen, R.D. 1983, The atmospheric lifetime experiment. 3. Lifetime methodology and application to three years of $CFCl_3$ data. J. Geophys. Res. 88C 8379-8400.

Derwent, R.G. and Curtis, A.R. 1977, Two-dimensional model studies of some trace gases and free radicals in the troposphere. Report AERE-R 8853 (U.K. Atomic Energy Authority, Harwell) 57pp.

Enting, I.G. 1982, Nuclear Weapons Data for Use in Carbon Cycle Modelling. Division of Atmospheric Physics, Technical Paper no. 44. (CSIRO, Australia) 18pp.

Enting, I.G. 1984, Techniques for Determining Surface Sources from Surface Observations of Atmospheric Constituents. CSIRO Division of Atmospheric Research, Technical Paper No. 5. (CSIRO, Australia) 30pp.

Enting, I.G. 1985a, Principles of constrained inversion in the calibration of carbon cycle modelling. Tellus 37B 7-27.

Enting, I.G. 1985b, A classification of some inverse problems in geochemical modelling. Tellus 37B 216-229.

Enting, I.G. and Mansbridge, J.V. 1986, Description of a two-dimensional atmospheric transport model. Division of Atmospheric Research Technical Paper No.11 (CSIRO).

Enting, I.G. and Pearman, G.I. 1986, The use of observations in calibrating and validating carbon cycle models. pp 425-458 of The Changing Carbon Cycle: A Global Analysis, (ed. J. Trabalka and D. Reichle), proceedings of the 6th Oak Ridge National Laboratory Life Sciences Symposium Knoxville Tennessee, 1983. (Springer-Verlag, New York).

Fishman, J., Solomon, S., and Crutzen, P. 1979, Observational and theoretical evidence in support of a significant in-situ photochemical source of tropospheric ozone. Tellus 31 432-446.

Fung, I. 1985, Analysis of the seasonal and geographical patterns of atmospheric $CO_2$ distributions with 3-D tracer model. pp.459-473 of "The Changing Carbon Cycle: A Global Analysis" proceedings of the 6th Oak Ridge National Laboratory Life Sciences Symposium. Knoxville, Tennessee, Oct. 31 Nov. 2, 1983. (Springer-Verlag, New York).

Fung, I., Prentice, K., Matthews, E., Lerner, J. and Russell, G. 1983, Three-dimensional tracer model study of atmospheric $CO_2$: Response to seasonal exchanges with the terrestrial biosphere. J. Geophys. Res. 88C 1281-1294.

Fung, I.Y., Tucker, C.J. and Prentice, K.C. 1985, On the variability of $CO_2$ exchange between the atmosphere and the biosphere. Presented at CSIRO-ABM workshop on 'The Scientific Application of Baseline Observations of Atmospheric Composition' 7-9 November 1984.

Gidel, L.T., Crutzen, P.J. and Fishman, J. 1983, A two-dimensional photochemical model of the atmosphere. 1: Chlorocarbon emissions and their effect on stratospheric ozone. J. Geophys. Res. 88C 6622-6640.

Harris, J.M. and Bodhaine, B.A. 1983, Geophysical Monitoring for Climatic Change No. 11. Summary Report 1982 (U.S. Dept. Commerce) 160pp.

Hidalgo. H. and Crutzen, P.J. 1977, The tropospheric and stratospheric composition perturbed by $NO_x$ emissions of high altitude aircraft. J. Geophys. Res. 82 5833-5866.

Holton, J.R. 1981, An advective model for two-dimensional transport of stratospheric trace species J. Geophys. Res. 86 11989-11994.

Hunten, D.M., 1975, Vertical transport in atmospheres. pp. 59-72 of Atmospheres of Earth and Planets ed. B.M. McCormax. D. Reidel (Hingham, Mass.)

Hyson, P., Fraser, P.J. and Pearman, G.I. 1980, A two-dimensional transport simulation model for trace atmospheric constituents. J. Geophys. Res. 85C 4443-4455.

Isaksen, I. and Rodhe, H. 1978, A two-dimensional model for the global distribution of gases and aerosol particles in the troposphere. Report AC-47 Department of meteorology (University of Stockholm) 36pp.

Karol, I.L., 1970, Numerical model of the global transport of radioactive tracers from the instantaneous sources in the lower stratosphere. J.Geophys.Res. 75 3589-3603.

Lanczos, C., 1966, A Discourse on Fourier Series. Oliver and Boyd (Edinburgh) 255 pp.

Levy, H., Mahlman, J.D. and Moxim, W.J. 1979, A preliminary report on the numerical simulation of the three-dimensional structure and variability of atmospheric $N_2O$. Geophys. Res. Lett. 6 155-158.

Louis, J.F. 1974, A two-dimensional transport model of the atmosphere. Ph.D. Thesis, University of Colorado.

Louis, J.F. 1975, pp6-23 to 6-31 and pp6-39 to 6-49 of The natural stratosphere of 1974. CIAP monograph 1. (Institute for defense analysis) about 1400pp.

Lowe, D.C., Guenther, P.R. and Keeling, C.D. 1979, The concentration of atmospheric carbon dioxide at Baring Head, New Zealand. Tellus 31 58-67.

Luther, F.M., 1975, pp6-31 to 6-38 of The natural stratosphere of 1974. CIAP monograph 1. (Institute for defense analysis) about 1400pp.

Mahlman, J.D. and Moxim, W.J. 1978, Tracer simulation using a global general circulation model: Results from a midlatitude instantaneous source experiment. J. Atmos. Sci. 35 1340-1374.

Matsuno, T. 1980, Lagrangian motion of air parcels in the stratosphere in the presence of planetary waves. Pure. Appl. Geophys. 118 189-216.

Miller, C., Filkin, D.L., Owens, A.J., Steed, J.M. and Jesson, J.P. 1981, A two-dimensional model of stratospheric chemistry and transport. J. Geophys. Res. 86C 12039-12065.

Mook, W.G., Koopmans, M., Carter, A.F. and Keeling, C.D. 1983, Seasonal, latitudinal, and secular variations in the abundance and isotopic ratios of atmospheric carbon dioxide. 1. Results from land stations. J. Geophys. Res. 88C 10915-10933.

Munnich, K.D. and Vogel, J.C., 1963., Investigation of meridional transport in the troposphere by means of carbon-14 measurements. pp 189-197 of Radioactive Dating. IAEA (Vienna).

Murgatroyd, R.J. and Singleton, F. 1961, Possible meridional circulations in the stratosphere and mesosphere. Quart.J. Roy. Meteor. Soc. 87 125-135.

Newell, R.E., Kidson, J.W., Vincent, D.J. and Boer, G.J. 1972, The General Circulation of the Tropical Atmosphere and Interactions with Extra-tropical Latitudes. (M.I.T. press) 258pp.

Noye, J. 1982, Finite difference methods for partial differential equations. pp3-137 of Numerical Solution of Partial Differential Equations. Proceedings of the 1981 Conference on Numerical Solutions of Partial Differential Equations, ed. J. Noye,Melbourne University 23-27 Aug. 1981 (North Holland, Amsterdam) 647pp.

Nydal, R. and Lovseth, K. 1983, Tracing Bomb $^{14}C$ in the atmosphere 1962-1980. J. Geophys. Res. 88C 3621-3642.

Oort, A.H. 1983, Global Atmospheric Circulation Statistics, 1958-1973. NOAA Professional Paper 14. (U.S. Dept. Commerce) 180pp plus microfiche.

Oort, A.H. and Rasmusson, E.M. 1971, Atmospheric Circulation Statistics, NOAA Professional Paper 5. (U.S. Govt Printing Office, Washington, D.C.) 323pp.

Pavlis, G.L. and Booker, J.R. 1980, The mixed discrete-continuous inverse problem: application to the simultaneous determination of earthquake hypocentres and velocity structure. J. Geophys. Res. 85B 4801-4810.

Pearman, G.I. and Beardsmore, D.J. 1984, Atmospheric carbon dioxide measurements in the Australian region: Ten years of aircraft data. Tellus 36B 1-24.

Pearman, G.I. and Hyson, P., 1980, Activities of the global biosphere as reflected in atmospheric $CO_2$ records. J. Geophys. Res. 85C 4457-4467.

Pearman, G.I. and Hyson, P. 1986, Global transport and interreservoir exchange of carbon dioxide with particular reference to stable isotopic distributions. J.Atmos.Chem.4 81-124.

Pearman, G.I., Hyson, P. and Fraser, P.J. 1983, The global distribution of atmospheric carbon dioxide: 1. Aspects of observations and modelling. J. Geophys. Res. 88C 3581-3590.

Peters, L.K. and Carmichael, G.R., 1984, Modelling of transport and chemical processes that affect regional and global distributions of trace species in the troposphere. pp493-538 of Trace Atmospheric Constituents: Properties, Transformations and Fates. ed. S.E. Schwartz. John Wiley and Sons. (NY). 547pp.

Peterson, K.R., 1970, An empirical model for estimating worldwide deposition from atmospheric nuclear detonations. Health Physics 18 357.

Pittock, A.B. 1983, The atmospheric effects of nuclear war. pp136-160 of Australia and Nuclear war. ed. M. Denborough. (Croom Helm, Fyshwick, ACT). 270pp.

Plumb, R.A. 1979, Eddy fluxes of conserved quantities by small-amplitude waves. J. Atmos. Sci. 36 1699-1704.

Plumb, R.A. 1985, The zonally-averaged transport characteristics of a GCM and a test of the validity of K-theory as a parameterization of eddy transport. Presented at CSIRO-ABM workshop on 'The Scientific Application of Baseline Observations of Atmospheric Composition', Aspendale, 7-9 November 1984.

Plumb, R.A. and Mahlman, J.D. 1987, The zonally-averaged transport characteristics of a GCM. J. Atmos. Sci. (in press).

Prather, M. 1985, Simulations of chlorofluorocarbons with a three dimensional model. Presented at CSIRO-ABM workshop on 'The Scientific Application of Baseline Observations of Atmospheric Composition, Aspendale, 7-9 November 1984.

Prinn, R.G. and Golombek, A. 1985, A global three-dimensional model of the circulation and chemistry of $CFCl_3$, $CF_2Cl_2$, $CH_3CCl_3$, $CCl_4$ and $N_2O$. Presented at CSIRO-ABM workshop on 'The Scientific Application of Baseline Observations of Atmospheric Composition',Aspendale, 7-9 November, 1984.

Pyle, J.A. and Rogers, C.F. 1980, Stratospheric transport by stationary planetary waves - The importance of chemical processes. Quart.J.R. Meteor. Soc. 106 421-446.

Rasmussen, R.A. and Lovelock, J.E. 1983, The atmospheric lifetime experiment. 2. Calibration. J. Geophys. Res. 88C 8369-8378.

Reed, R.J. and German, K.E. 1965, A contribution to the problem of stratospheric diffusion by large-scale mixing. Mon. Weather. Rev. 93 313-321.

Reiter, E.R. 1978, Atmospheric Transport Processes. part 4: Radioactive Tracers. (U.S. Dept. of Energy) 608pp.

Rodhe, H. and Isaksen, I. 1980, Global distribution of sulfur compounds in the troposphere estimated in a height/latitude transport model. J. Geophys. Res., 85C 7401-7409.

Rotty, R.M. 1983, Distribution of and changes in industrial carbon dioxide production. J. Geophys. Res. 88C 1301-1308.

Tanaka, M., Nakazawa, T. and Aoki, S., 1983, Concentration of atmospheric carbon dioxide over Japan. J.Geophys.Res. 88C 1339-1344.

Tans, P. 1981, A compilation of bomb $^{14}C$ data for use in global carbon model calculations. pp131-157 of Carbon Cycle Modelling. SCOPE16. ed. B. Bolin. (John Wiley and Sons, Chichester).

Thompson, M.L., Enting, I.G., Pearman, G.I., and Hyson, P. 1986, Interannual variations of atmospheric $CO_2$ concentration. J.Atmos.Chem.4 125-55.

Wallace, J.M. 1978, Trajectory slopes, countergradient heat fluxes and mixing by lower stratospheric waves. J. Atmos. Sci. 35 554-558.

Whitten, R.C., Borucki, W.J., Watson, V.R., Shimazaki, T., Woodward, H.T., Riegel C.A., Capone, L.A. and Becker, T. 1977, The NASA Ames research centre one-and two-dimensional stratospheric models, part ii. The two-dimensional model. NASA Technical paper 1003.

Widhopf, G.F. and Giatt, L. 1980, The aerospace time dependent 2-dimensional photochemical model of the atmosphere. Presented at WMO workshop on two-dimensional modelling. Toronto, 1980.

Wiggins, R. 1972, The general linear inverse problem: implications of surface waves and free oscillations on earth structure. Rev. Geophys. Space Phys. 10 251-285.

Wong, C.S., Bellegay, R.D. and Page, J.S. 1981, Seasonal and large-scale variabilities of atmospheric carbon dioxide over North Pacific Ocean. pp43-49 of Papers presented at the WMO/ICSU/UNEP Scientific Conference on Analysis and Interpretation of atmospheric $CO_2$ data. Bern, 14-18 September 1981.

Wong, C.S. and Pettit, K.G. 1981, Global-scale secular $CO_2$ trends and seasonal changes at Canadian $CO_2$ stations; Ocean weather station P, Sable Island and Alert. pp35-42 of Papers presented at the WMO/ICSU/UNEP Scientific Conference on Analysis and Interpretation of Atmospheric $CO_2$ data. Bern, 14-18 September 1981.

Wunsch, C. 1978, The North Atlantic general circulation west of 50W determined by inverse methods. Rev. Geophys. Space Phys. 16 583-620.

Wunsch, C. and Minster, J.-F. 1982, Methods for box models and ocean circulation tracers: Mathematical programming and non-linear inverse theory. J. Geophys. Res. 87C 5647-5662.

Young, J.A., Erickson, N.E. and Fairhall, A.W. 1965, Tropospheric $^{14}C$ values in the Pacific Northwest and the Arctic basin during 1964. pp 422-427 of Radioactive Fallout from Nuclear Weapons. ed. A.W. Klement. (USAEC) 953pp.

Young, J.A. and Fairhall, A.W. 1968, Radiocarbon from nuclear weapons tests. J. Geophys. Res. 73 1185-1200.